MEASURING ACTIVATION OF THE CYTOSOLIC DNA SENSING PATHWAY

APPROVED BY SUPERVISORY COMMITTEE

Dr. Zhijian 'James' Chen

Dr. Bruce A. Beutler

Dr. Melanie H. Cobb

Dr. Benjamin P. Tu (Chair)

DEDICATION

I would like to thank my mentor, Dr. Zhijian 'James' Chen, for his guidance, advice, and patience throughout my Ph.D. I am so grateful for the opportunity to be part of his lab and learn from him. I would like to thank my lab members for their assistance, discussion, and friendship. I also want to thank my collaborators, for their essential contributions to my project. Finally, I would like to thank my friends and family, for their unwavering support throughout my years in the MSTP.

MEASURING ACTIVATION OF THE CYTOSOLIC DNA SENSING PATHWAY

By

NICOLE L VARNADO

DISSERTATION

Presented to the Faculty of the Graduate School of Biomedical Sciences

The University of Texas Southwestern Medical Center at Dallas

In Partial Fulfillment of the Requirements

For the Degree of

DOCTOR OF PHILOSOPHY

The University of Texas Southwestern Medical Center at Dallas

Dallas, Texas

May, 2019

Copyright

by

NICOLE L VARNADO, 2019

All Rights Reserved

MEASURING ACTIVATION OF THE CYTOSOLIC DNA SENSING PATHWAY

Publication No. _____

NICOLE L VARNADO, M.D., Ph.D.

The University of Texas Southwestern Medical Center at Dallas, 2019

Supervising Professor: Zhijian 'James' Chen, Ph.D.

In mammalian cells, DNA is normally sequestered within the confines of the nucleus or mitochondria. Entrance of DNA into the cytosol, whether foreign or self in origin, acts as a danger signal that triggers a host innate immune response.

Cytosolically localized DNA is sensed by cyclic GMP-AMP synthase (cGAS), which synthesizes a novel second messenger known as cyclic GMP-AMP (2'3'-cGAMP). 2'3'-cGAMP, in turn, binds to and activates the ER resident adaptor Stimulator of Interferon Genes (STING), which triggers downstream signaling that culminates in the production of type-I interferons and other immune modulatory molecules.

The pathway underlies the recognition of pathogenic DNA necessary to quell microbial infections, as well as the aberrant detection of self-DNA responsible for inducing certain autoimmune diseases. Such appreciation for the involvement of cGAS-cGAMP-STING signaling

in numerous clinical phenotypes necessitates development of tools that can outline the extent of its contribution to various diseases. Additionally, numerous questions remain regarding the regulation of cGAS-cGAMP signaling.

As 2'3'-cGAMP production is a hallmark of the pathway's activation, we sought to develop a robust method to monitor its formation *in vivo*, and quantify its levels in a wide variety of settings. Herein we present the development of an antibody of high sensitivity and specificity for this small molecule second messenger, capable of recognizing and quantifying 2'3'-cGAMP production *in vivo*. We show it can be adapted for use in a variety of techniques, to track and measure levels of 2'3'-cGAMP quantitatively, to visualize 2'3'-cGAMP produced in cells, and to quickly identify cGAMP-positive cell populations within live samples. We show this antibody to be an invaluable tool to elucidate outstanding questions in the field, and demonstrate its potential to detect patients with aberrant activation of the cGAS-STING pathway. We foresee a future in which the 2'3'-cGAMP antibody is used to quantify activation of the cGAS pathway in a variety of clinical and research settings.

TABLE OF CONTENTS

PRIOR PUBLICATIONS

Mace, D. L., **Varnado, N**., Zhang, W., Frise, E., & Ohler, U. (2010). Extraction and comparison of gene expression patterns from 2D RNA in situ hybridization images. *Bioinformatics, 26*(6), 761-769.

LIST OF FIGURES

CHAPTER I
Introduction

Pathogen recognition by the innate immune system

There are two arms to the vertebrate immune system, the innate and the adaptive components (Janeway & Medzhitov, 2002). While the innate immune system is an evolutionarily ancient defense mechanism found in both plants and animals, the adaptive immune system developed relatively recently and is known to exist only in vertebrates. The two systems differ widely in their timing, distribution, and specificity – differences attributed largely to the receptors employed by each for pathogen detection.

The adaptive immune system is the slower, but more specific component of immunity, acting on the order of days after an infection (Bonilla & Oettgen, 2010). It employs B-cells, which are involved in antibody production, and T-cells, which generate a cell-mediated response. These lymphocytes contain receptors encoded in gene segments, which randomly rearrange during development and provide each cell with a unique receptor specific to a single antigen (Tonegawa, 1983). This affords the host an expansive array of antigen receptors. Lymphocytes that encounter their specified antigen will become activated and undergo clonal expansion. This process of lymphocyte activation, proliferation, and differentiation to effector cells requires multiple days and accounts for the delayed response of the adaptive system. Although the response to a specific pathogen ultimately subsides, some antigen-specific cells remain within the host, acting as a lasting immunological memory for any subsequent infection by the pathogen (Ahmed & Gray, 1996).

Conversely, the innate immune system represents the host's first line of defense against pathogen invasion, serving to rapidly contain infection and, crucially, initiate and direct the adaptive immune system (Kawai & Akira, 2009). Its receptors, known as pattern recognition

receptors (PRRs) are germ-line encoded - selected for over time to recognize those microbial components conserved among large arrays of pathogens (known as pathogen associated molecular patterns, or PAMPs).

Among the first PRRs discovered were members of the Toll-like receptor (TLR) family, and recognized PAMPS exclusive to microbes, such as LPS (by TLR4), bacterial lipopeptides (by TLR1/2/6), and flagellin (by TLR5) (Hayashi et al., 2001; M. S. Jin et al., 2007; O'Neill, Golenbock, & Bowie, 2013; Poltorak et al., 1998; Takeuchi et al., 2001; Takeuchi et al., 2002). However, other subsequently identified TLRs were found to bind nucleic acids, which expanded the list of PAMPs (and pathogens detectable by the innate immune system), and raised the question of how these PRRs might distinguish their ligands from host material (Gurtler & Bowie, 2013). These nucleic acid TLRs included TLR3, which binds double-stranded RNA, TLR7 and 8, which bind single-stranded RNA, TLR9, which binds unmethylated CpG DNA from bacteria, and TLR13, which recognizes a specific sequence in the 23S ribosomal RNA of bacteria (Alexopoulou, Holt, Medzhitov, & Flavell, 2001; Diebold, Kaisho, Hemmi, Akira, & Reis e Sousa, 2004; Heil et al., 2004; Hemmi et al., 2000; X. D. Li & Chen, 2012; Lund et al., 2004).

While some members of the TLR family are expressed on the cell surface, the nucleic acid sensing TLRs (TLR3, 7, 8, 9, and 13) were found to localize to the endosomal membrane, thereby allowing surveillance of endosomes and lysosomes (Ahmad-Nejad et al., 2002; Nishiya & DeFranco, 2004). However, these receptors could not account for detection of nucleic acids exposed to the cytoplasm, whether self or non-self in origin.

Soon after these discoveries, two PRRs, RIG-I and MDA5, were identified to bind double-stranded RNA in the cytoplasm and trigger the type I interferon pathway (Crowl, Gray, Pestal, Volkman, & Stetson, 2017). These cytoplasmically localized RNA helicases were found

to detect infection of cells by multiple RNA viruses, and initiate production of type I interferons (IFNs). With TLR9 as the only identified DNA-binding PRR, only capable of recognizing a bacterial component, and only localized to the endosomal compartment, the question remained: what is the sensor of cytosolic DNA?

Detection of cytosolic DNA by the innate immune system

It should be noted that the TLRs are restricted in their expression to only a subset of cell types, namely specific immune cells. The endosomal DNA sensor TLR9 is preferentially expressed in plasmacytoid dendritic cells, as well as monocytes/macrophages, B-cells and T-cells (Hornung et al., 2002; Kadowaki et al., 2001). Upon its activation, TLR9 signals through an adaptor protein, MyD88, to activate type I IFN production (Hacker et al., 2000). However, soon after the discovery of TLR9, multiple studies found that certain DNA viruses and bacteria can incite type I IFN production independent of TLR9 and MyD88, and that recognition of transfected synthetic DNA is also TLR9-independent (Ishii et al., 2006). These studies implied the existence not only of a unique cytoplasmic DNA sensor, but an entirely separate pathway downstream of the recognition event. Indeed, subsequent studies demonstrated the requirement of TANK-binding kinase (TBK1) and Interferon Regulatory Factor 3 (IRF3) for activation of type I IFN upon cytosolic DNA recognition (Ishii et al., 2006; Stetson & Medzhitov, 2006).

Soon after, several proteins were proposed to fill the role of cytosolic DNA sensor, including DAI/ZBP-1, IFI16, DDX41, DNA-PK, and AIM2. However, there is no strong genetic evidence to support a role of any of these protein as a cytosolic DNA sensor that triggers the type I IFN response (Vance, 2016).

A major advance came with the discovery of Stimulator of Interferon Genes (STING; also, MPYS/MITA/ERIS/TMEM173) (Ishikawa & Barber, 2008; L. Jin et al., 2008; W. Sun et

al., 2009; Zhong et al., 2008). STING was found to be essential for the type I IFN response to cytosolic DNA, as cells deficient in STING cannot mount an IFN response to dsDNA treatment (Ishikawa, Ma, & Barber, 2009). However, STING is not a sensor of cytosolic DNA but rather an adaptor protein that mediates the activation of IRF3 in response to DNA stimulation.

Finally, through a series of biochemical studies completed in our lab, one protein emerged as essential for recognition of cytosolic DNA and subsequent type I IFN induction: cyclic GMP-AMP synthase, or cGAS (L. Sun, Wu, Du, Chen, & Chen, 2013; J. Wu et al., 2013). Surprisingly, cGAS acts not only as a DNA sensor, but also as a synthetic enzyme. As a direct result of dsDNA binding, cGAS synthesizes a small molecule second messenger, and it is this small molecule that directly binds and activates downstream adaptor STING. In fact, cGAS was only identified after discovery of the second messenger, which was found using an *in vitro* complementation assay: cells lacking STING were treated with various forms of dsDNA, and the resulting cytoplasmic extracts were incubated with perfringolysin O (PFO)-permeabilized cells to allow cytoplasmic mixing. Presumably, any upstream activator of STING from the dsDNA-treated cells should stimulate STING from the permeabilized cells, and lead to downstream pathway activation (i.e. IRF3 dimerization). The activing molecule was surprisingly heat-, benzonase-, and proteinase K- resistant, thus excluding the possibility of a protein, DNA, or RNA activator. Using a series of biochemical purification steps coupled with Nano liquid chromatography-mass spectrometry (LC-MS), the mysterious activator was identified as a small molecule composed of AMP and GMP residues linked by phosphodiester bonds: cyclic GMP-AMP (cGAMP). cGAMP acts as a second messenger in the pathway: its direct binding to STING propagates the initial recognition of dsDNA by its upstream sensor. This finding, although surprising, was consistent with existing knowledge that STING could bind to similarly structured

small molecules known as cyclic dinucleotides (CDNs, discussed below) (Burdette et al., 2011; Huang, Liu, Du, Jiang, & Su, 2012; Ouyang et al., 2012; Shang et al., 2012; Shu, Yi, Watts, Kao, & Li, 2012; Yin et al., 2012).

Figure 1 provides a schematic overview of the cytosolic DNA sensing pathway. To summarize our current knowledge: cGAS normally resides within the cytoplasm in its apo-form, or auto-inhibited state (Civril et al., 2013; P. Gao et al., 2013; Kranzusch, Lee, Berger, & Doudna, 2013; X. Li et al., 2013; X. Zhang et al., 2014). When dsDNA enters into the cytoplasm, whether foreign or self in origin, it is directly bound by cGAS at its sugar phosphate backbone, independent of sequence. This occurs in a 2:2 fashion: a complex is formed containing two molecules of cGAS bound to two molecules of dsDNA (X. Li et al., 2013; X. Zhang et al., 2014). This binding event initiates a conformational change in the active site of cGAS, allowing synthesis of cGAMP from one molecule of GTP and one molecule of ATP. cGAMP then acts as a second messenger, traversing the cytoplasm and binding directly to ER-localized STING (J. Wu et al., 2013; Zhang et al., 2013). cGAMP binding to STING triggers a conformational change in STING, allowing it to traffic through the Golgi apparatus to a perinuclear location, where it forms distinct puncta (Dobbs et al., 2015; Ishikawa et al., 2009; Saitoh et al., 2009). STING then recruits and activates the kinase TBK1 (as well as kinase IKK), which subsequently activates the transcription factor IRF3 (and transcription factor Nf-κB) through direct phosphorylation (Tanaka & Chen, 2012). IRF3 can then dimerize, enter the nucleus, and induce expression of type I IFNs (along with other key innate immune signaling molecules).

Subsequent studies demonstrated the clinical importance of the cGAS-STING pathway: it was shown to be essential for detection of numerous pathogens, as well as aberrantly localized host DNA (discussed below).

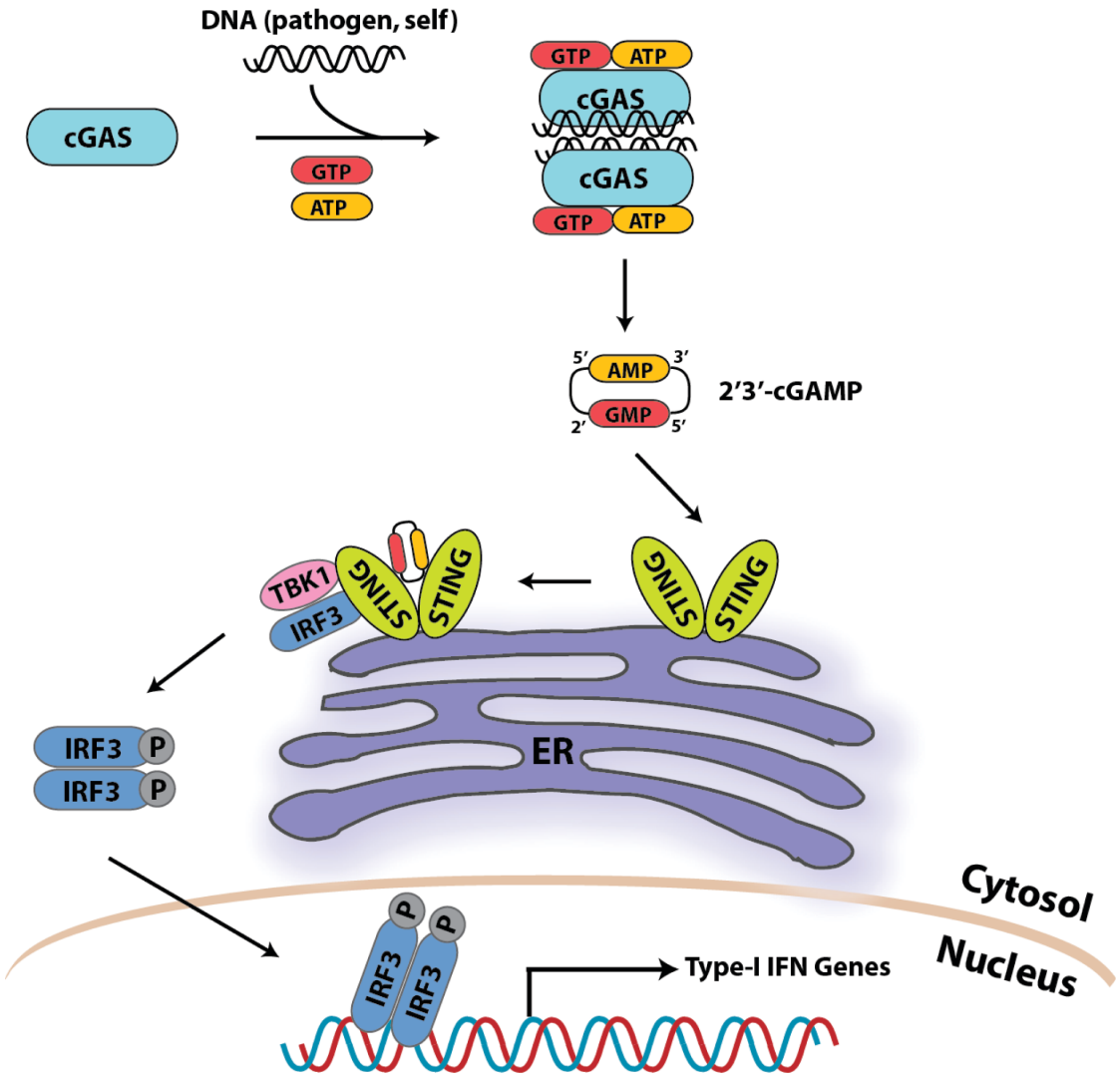

Figure 1. Overview of the Cytosolic DNA Sensing Pathway.
Adapted with permission from Dr. Jiaxi Wu (created by Dr. Wu and Nicole Varnado).

2’3’-cGAMP and other cyclic dinucleotides

cGAMP is quite a unique small molecule. It is the first and only cyclic dinucleotide identified in metazoans, joining a small but well-studied family of second messenger signaling molecules found in bacteria.

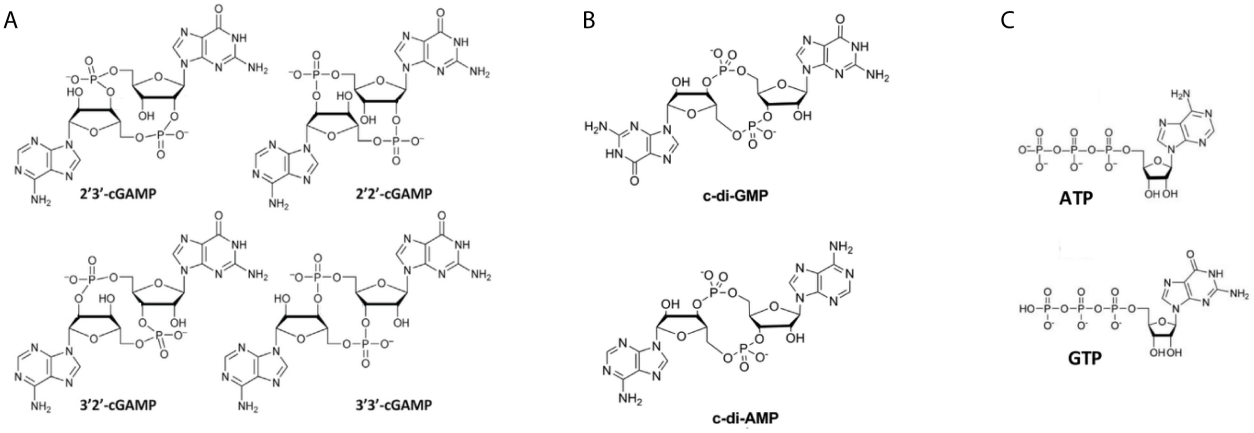

Figure 2. Small Molecules Related to 2’3’-cGAMP.
(A) Chemical structures of the possible isomers of cGAMP, depending on the combination of phosphodiester bonds linking together the two nucleoside residues. (B) Chemical structures of cyclic-di-GMP and cyclic-di-AMP, members of the cyclic dinucleotide (CDN) class synthesized by bacteria (and archaea, in the case of cyclic-di-AMP). (C) Chemical structures of Adenosine triphosphate (ATP) and Guanosine triphosphate (GTP), components of the CDNs.

Figure 2 shows all currently identified cyclic dinucleotides (CDNs). They share a common overall structure: two purine residues linked by two phosphodiester bonds. The first to be discovered, in 1987, was bacterial cyclic-di-GMP (cdG) – this is by far the most studied and well-characterized of the CDNs (Ross et al., 1987). Indeed, extensive work over the last three decades has established cdG as a universal signaling molecule in bacteria, as it is found within all the major bacterial lineages (Jenal, Reinders, & Lori, 2017). It plays a wide variety of roles (a

description of which is outside the scope of this manuscript), although it is most widely used for establishing biofilms and regulating the motile-sessile transition of bacteria (Jenal et al., 2017).

The second CDN to be discovered was cyclic-di-AMP (cdA), which is also found in a variety of bacteria and archaea (Witte, Hartung, Buttner, & Hopfner, 2008). Multiple functions have been defined for cdA, including its role in maintaining DNA integrity and membrane lipid homeostasis (Corrigan & Grundling, 2013). Because it was discovered relatively recently, further study is needed to determine the extent of its distribution in organisms, as well as additional roles it may play.

cdG and cdA are structurally most similar: both contain two of the same nucleotide, and both are connected by identical phosphodiester linkages using the 3' hydroxyl moiety of the first nucleotide and 5' phosphate moiety of the second nucleotide (hence the designation 3',3'-). Bacterial cyclic-GMP-AMP, or 3'3'-cGAMP, contains the same phosphodiester linkages as cdG and cdA, but is made up of mixed nucleotide residues. It was first identified in the bacteria, *Vibrio cholera*, where it is used to control colonization and virulence of the organism (Davies, Bogard, Young, & Mekalanos, 2012). More recently, two studies have outlined a novel role for 3'3'-cGAMP in various members of the Proteobacteria class, Deltaproteobacteria (Hallberg et al., 2016). Another recent study identified a 3'3'-cGAMP molecule produced by anemone cGAS and capable of binding to anemone STING (Kranzusch et al., 2015).

With the discovery of cGAS in 2013 came the final known member of the CDN family, 2'3'-cGAMP (L. Sun et al., 2013; J. Wu et al., 2013). 2'3'-cGAMP is the most unique CDN in both its structure and function. In addition to containing mixed nucleotides, it was found to contain mixed phosphodiester linkages – one of which utilizes the 2' hydroxyl residue of GMP (Ablasser, Goldeck, et al., 2013; Diner et al., 2013; P. Gao et al., 2013; Zhang et al., 2013). It

should be noted that three additional cGAMP isomers can be synthesized from the other possible combinations of linkages, but 2'3'-cGAMP is the only isomer produced endogenously by cGAS. Interestingly, all four isomers are capable of inducing IFN-β production when used to stimulate the downstream adaptor STING, although 2'3'-cGAMP binds the adaptor with much greater affinity than the other isomers.

2'3'-cGAMP has been studied most in the context of cytosolic DNA sensing (as described above). Structural studies have clearly defined the binding of 2'3'-cGAMP to the downstream adaptor protein STING, proving its role as a second messenger signaling molecule within the innate immune system. A potentially new role for 2'3'-cGAMP was recently proposed: a study published in 2014 claimed that all four naturally occurring cyclic dinucleotides are capable of binding a hyperpolarization-activated cyclic nucleotide-gated (HCN) channel, which controls the I_f current within pacemaker cardiac myocytes (Lolicato et al., 2014). However, a more complete study involving structural experiments is necessary to verify 2'3'-cGAMP binding to HCNs.

Despite a similar structure, the individual CDNs are synthesized, regulated, and degraded by distinct enzymes. cdG can be synthesized by many different bacterial enzymes known as diguanylate cyclases (found across all bacterial phyla), and cyclic-di-AMP (cdA) by multiple diadenylyl cyclases (Krasteva & Sondermann, 2017). DncV, an enzyme found in *V. cholera*, is responsible for bacterial cGAMP (3'3'-cGAMP) synthesis, although a recent report found that a subset of bacterial enzymes containing a domain used for cdG synthesis (the GGDEF domain) can also synthesize 3'3'-cGAMP (Hallberg et al., 2016). Based on our current knowledge, cGAS is the only enzyme capable of synthesizing metazoan 2'3'-cGAMP.

There are also transport mechanisms in place for certain CDNs to move across membranes, between cells, or out of cells. For example, the pathogenic bacteria *Listeria monocytogenes*, uses a multidrug efflux pump (MDR) system to export cdA from the organism (which can subsequently activate STING and IFN production in the host) (Woodward, Iavarone, & Portnoy, 2010). Although there is no identified mechanism for direct export of 2'3'-cGAMP into the extracellular space, several recent studies have observed the transfer of 2'3'-cGAMP between cells. One study showed that 2'3'-cGAMP moves from infected cells to bystander cells via gap junctions, allowing activation of bystander cell STING (Ablasser, Schmid-Burgk, et al., 2013). Two more recent concurrently published studies demonstrated that virally infected cells can package 2'3'-cGAMP into viral progeny, which spreads antiviral signaling to subsequently infected cells. These findings all establish mechanisms to propagate antiviral signaling from pathogen-infected cells (Bridgeman et al., 2015; Gentili et al., 2015).

CDNs are also known to be degraded in certain contexts by enzymes known as phosphodiesterases (PDEs). Specific CDNs are degraded by PDE families that have the appropriate hydrolysis domain for that CDN. cdA and cdG have numerous specific PDEs, some of which are localized extracellularly to degrade CDNs outside of bacteria. Currently there are no known bacterial cGAMP PDEs. Only one PDE is reported to degrade metazoan 2'3'-cGAMP, known as ecto-nucleotide pyrophosphatase/phosphodiesterase (ENPP1) (L. Li et al., 2014). As an ectoenzyme, ENPP1's catalytic domain and thus activity is located extracellularly, and it can also be shed into the extracellular space. Indeed, this study found ENPP1 hydrolase activity in human sera samples. As mentioned above, there are no known mechanisms to pump or transport 2'3'-cGAMP out of cells, but the existence of an extracellular PDE does posit the presence of extracellular 2'3'-cGAMP. It remains to be seen whether a system exists intracellularly to

degrade or remove 2'3'-cGAMP. Additionally, a group discovered that a PDE – CdnP - from the bacteria *Mycobacterium tuberculosis* can degrade metazoan 2'3'-cGAMP *in vitro*, and *ex vivo* in infected macrophages (Dey et al., 2017).

The role of cytosolic DNA sensing in disease

Based on our current understanding of the cGAS-cGAMP-STING pathway, one can imagine numerous clinical scenarios in which the pathway is necessary for an appropriate host immune response. The first and most obvious is detection and defense against pathogens. Conversely, activation of this pathway at inappropriate times could lead to an inflammatory phenotype. For example, self-DNA is normally compartmentalized within the nucleus or the mitochondria, and if it happens to leak out there are numerous cytoplasmic DNases in place to degrade such DNA. But when these mechanisms fail, this pathway could be stimulated and lead to autoimmune disease. Similarly, if any component of this pathway were to harbor an autoactive mutation, it could also be detrimental for the host. A final and somewhat surprising area of medicine affected by the cytosolic DNA sensing pathway is oncology, as recent but well-accepted studies highlight the pathway's importance in cancer immunogenicity and immunotherapy.

Infectious diseases

The in vivo significance of cGAS-cGAMP-STING signaling in host defense has been validated in several recent studies. This pathway is essential for detection of multiple microbes, and is implicated in detection of an even broader spectrum of organisms.

Through genetic deletion studies, it has been shown that when mice or cells lack cGAS or STING, they bear higher titers of the infectious agent, produce less type I IFNs, and succumb more readily to disease. Such infectious agents include multiple DNA viruses that infect humans,

including Vaccinia Virus (VV), Herpes Simplex Virus 1 (HSV-1), Human Cytomegalovirus (HCMV), and Kaposi's sarcoma-associated herpesvirus (KSHV) (D. Gao et al., 2013; X. D. Li et al., 2013; Lio et al., 2016; Paijo et al., 2016; Schoggins et al., 2014; J. J. Wu et al., 2015). The pathway is also required for detection of some retroviruses, including Human Immunodeficiency Virus (HIV) (D. Gao et al., 2013).

Additional genetic deletion studies showed that the pathway is required for detection of multiple pathogenic bacteria that contain DNA, most notably *Mycobacterium tuberculosis* (the causative agent of Tuberculosis or TB), *Francisella novicida*, *Neisseria gonorrhoeae*, and Group B *Streptococcus* (Andrade, Agarwal, et al., 2016; Andrade, Firon, et al., 2016; Collins et al., 2015; Storek, Gertsvolf, Ohlson, & Monack, 2015; Wassermann et al., 2015; Watson et al., 2015). The pathway is also required for detection of parasites, including *Plasmodium yoelii*, the causative agent of the disease malaria (Yu et al., 2016).

Several knockdown studies have suggested a role for cGAS-STING signaling in other infections, including infection by the viruses Hepatitis B (HBV) and Dengue Virus, and the bacterial pathogens *L. monocytogenes*, and *Chlamydia trachomatis* (Aguirre et al., 2017; Hansen et al., 2014; He et al., 2016; B. Sun et al., 2017; Y. Zhang et al., 2014). We believe this list will continue to grow as additional studies are published.

Autoimmune and Autoinflammatory diseases

As mentioned earlier, before the discovery of TLR9, the immune system's task of distinguishing self- from non-self seemed relatively straightforward, as the known PRRs recognized molecules unique to pathogens. With the discovery of cGAS and the other nucleic acid sensing PRRs, the potential arose for detection of endogenous molecules, and therefore inappropriate immune activity. As it turns out, there are critical mechanisms in place to

safeguard against PRR recognition of self-nucleic acids, and patients with errors in these mechanisms display autoimmune and autoinflammatory disease.

First and foremost, as a safeguard against erroneous detection, host DNA is normally sequestered within the nucleus or mitochondria. If DNA happens to escape these spaces, multiple nucleases are present to degrade the material. Those related to known clinical phenotypes include Trex1, a cytoplasmic 3'->5' DNA exonuclease, and RNaseH2 (all three subunits), a ribonuclease that hydrolyzes the RNA of RNA:DNA hybrids. A failure of these enzymes will lead to an accumulation of DNA within the cytoplasm, allowing for stimulation of the cGAS-STING pathway, and production of type I IFNs.

Several autoimmune/autoinflammatory disorders are, in fact, characterized by overproduction of type I IFNs – these are known as the type I interferonopathies (Crow, 2011). Patients with these disorders display phenotypes resulting from this elevated type I IFN production. Recent investigation into the molecular underpinnings of some of these disorders has demonstrated a clear role for cGAS-STING signaling in their pathology.

a. Acardi-Goutieres Syndrome (AGS). In this disorder, patients present at a young age with what appears to be a congenital viral infection: they have brain calcifications and brain inflammation, display psychomotor abnormalities (as a result of demyelination), have increased levels of lymphocytes in the CSF, and elevated levels of type I IFNs in serum and CSF (Aicardi & Goutieres, 1984). Detailed genetic analysis of families with AGS revealed the presence of inactivating mutations in the above-mentioned cytoplasmic nucleases, supporting the hypothesis that perhaps cGAS-STING signaling contributes to high IFN levels. It should be noted that mutation in other nucleases that regulate nucleic acid levels in the cytoplasm can also cause AGS, including SAMHD1, a dNTP triphosphohydrolase; ADAR1, an RNA-editing enzyme that

acts through deaminase activity; and MDA5, an RNA sensor mentioned in previous sections (Crow et al., 2015; Livingston & Crow, 2016).

Mice deficient in Trex1 display a similar autoinflammatory phenotype (which includes increased IFN signatures along with prominent myocarditis) and succumb rapidly to their disease (Morita et al., 2004). Importantly, this phenotype can be fully rescued by cGAS or STING knockout, demonstrating that cGAS-STING activity is responsible for autoinflammatory disease and death of the Trex1 deficient mice (Gao et al., 2015; Gray, Treuting, Woodward, & Stetson, 2015). Additionally, our lab detected increased levels of 2'3'-cGAMP in whole hearts of *Trex1*$^{-/-}$ and *Trex1*$^{-/-}$*STING*$^{-/-}$ mice (Gao et al., 2015). More recent genetic studies also found cGAS-STING signaling to be responsible for the IFN production and clinical phenotype of SAMHD1 and RNaseH2 deficient mice (Mackenzie et al., 2016; Maelfait, Bridgeman, Benlahrech, Cursi, & Rehwinkel, 2016).

b. Monogenic disorders caused by activating mutations in STING. Other disorders characterized by elevated type I IFN production can be explained by defects in components of the cGAS-STING pathway. A recent study centered around a small group of children with a systemic autoinflammatory system named STING-associated vasculopathy with onset in infancy (SAVI) (Liu et al., 2014). The patients displayed multiple clinical features resulting from vascular inflammation and damage including dermatological lesions and interstitial lung disease. Whole-exome sequencing of patients revealed three different *de novo* autosomal dominant mutations in STING, all leading to its constitutive activation and ultimately resulting in chronic increases in type I IFN production. The identified mutated amino acid residues are all located near STING's dimerization domain: N154S, V155M, and V147L.

A later study described a family with an inherited autosomal dominant mutation in STING, also resulting in the protein's auto-activation (Jeremiah et al., 2014). Like SAVI patients, these patients displayed elevated IFN levels and an inflammatory phenotype similar to that of lupus patients. Subsequent genetic analysis found the mutation to be identical to one of those found in SAVI patients, specifically V155M.

Finally, a third study identified a family with a heterozygous gain-of-function mutation in STING, who as a result had a disorder known as Familial chilblain lupus (a monogenic cutaneous lupus) (Konig et al., 2017). This mutation was G166E, which is unique relative to the above-mentioned studies, but all the mutations are near or within the dimerization domain of STING.

c. Systemic Lupus Erythematosus (SLE). Several recent reviews of the nucleic acid sensing field have suggested a potential role for cGAS-STING signaling in SLE (Crowl et al., 2017; Ding, Dong, Zhang, Ni, & Hou, 2015). SLE is a heterogeneous, multisystem autoimmune disease characterized by widespread tissue damage via immune complex deposition – it can affect many different organs and the degree of presentation can be mild to severe. Importantly, approximately two-thirds of SLE patients display elevated type I IFN signatures in their blood. This, combined with knowledge of the above monogenic disorders reminiscent of SLE presentations, supports the idea that cGAS-STING signaling may contribute to the disorder. A recent study of 50 SLE patients found cGAS expression in peripheral blood mononuclear cells (PBMCs) to be elevated relative to levels in normal patients (as a control, patients with Rheumatoid Arthritis, another autoimmune disease, did not show elevated cGAS expression levels) (An et al., 2017). Furthermore, out of 48 SLE patients, 15% showed elevated levels of 2'3'-cGAMP relative to levels in healthy counterparts (and RA patients).

Monitoring activity of the cytosolic DNA sensing pathway

The above-mentioned clinical relevance of the cGAS-cGAMP-STING pathway underscores a need to monitor its activation, regulation, and termination. Like many pathways in the innate immune system, its signaling ultimately leads to the production of type I IFNs and inflammatory cytokines such as IL-6, and IL-1β. Furthermore, some of its signaling components are shared by other PRRs systems, such as TBK1, IRF3, and NF-κB. It is thus difficult to tease apart and study the cGAS-cGAMP-STING pathway from other innate immune pathways.

Currently, pathway activity can be monitored in several ways including: type I IFN production (for example, IFNβ production measured by qPCR, ELISA, etc.), phosphorylation of pathway components (such as western blotting of p-TBK1, p-IRF3, etc.), dimerization of key transcription factors (such as IRF3), and immunostaining of adaptor protein STING to monitor trafficking and puncta formation (along with immunostaining of other proteins). These are sensitive and robust techniques when cells are stimulated specifically with dsDNA, and it can be assumed these measurements are a readout of cGAS' DNA sensing activity, but they are not actually specific to the pathway. This is more of a problem when trying to determine the contribution of cGAS-STING signaling to a given pathogen infection or autoimmune/autoinflammatory disease; in such cases, we need to detect a marker totally specific to the pathway. Because 2'3'-cGAMP is known to function only within this pathway, its detection is an optimal method to assess the pathway's regulation and contribution to disease.

There are currently few methods available for monitoring 2'3'-cGAMP levels, and each has limitations. Thin Layer Chromatography (TLC) can measure cGAMP levels *in vitro*, but it requires use of radioactive molecules and is only qualitative in its detection (Burhenne & Kaever, 2013). Our lab also developed another 'cGAMP activity assay': DNA-stimulated cells

are lysed and boiled, and the resulting heat-resistant supernatant is incubated with perfringolysin O (PFO)-permeabilized THP-1 or Raw264.7 cells (human monocytes and murine macrophages, respectively) – these cells are then assessed for IRF3 dimerization and therefore cGAMP production in the original stimulated cells (J. Wu et al., 2013). Again, this is only a qualitative measure, and is performed *in vitro*.

Liquid Chromatography – Mass Spectrometry (LC-MS) is a quantitative and highly sensitive technique now adapted for measuring 2'3'-cGAMP from cell line extracts, mouse tissue extracts, and extracts from PBMCs of lupus patients (An et al., 2017; Gao et al., 2015; Gray et al., 2015; J. Wu et al., 2013). However, LC-MS studies cannot be used to visualize 2'3'-cGAMP localization in cells or tissues, or for live-cell imaging/*in vivo* measurements. Furthermore, this process requires a high degree of expertise and training, is labor- and time-intensive, and involves use of large and expensive machinery, making it difficult to adapt for use in a clinical setting.

More recently, RNA-based fluorescent sensors were designed to bind and detect 2'3'-cGAMP (Bose, Su, Marcus, Raulet, & Hammond, 2016). The sensors are modified GEMM-II RNA riboswitch aptamers fused to a Spinach2 RNA aptamer – the riboswitch binds directly to 2'3'-cGAMP, which allows Spinach2 to bind/activate the fluorescent molecule DFHBI (Kellenberger, Wilson, Sales-Lee, & Hammond, 2013). One biosensor had a micromolar binding affinity to 2'3'-cGAMP (reported K_D of 13.4 ± 0.9 μM) – however, it had a higher binding affinity for cyclic-di-GMP (reported K_D of 0.021 ± 0.008 μM) and thus was not specific for 2'3'-cGAMP. The other biosensor was also not specific for 2'3'-cGAMP, and bound cyclic di-GMP and 3'3'-cGAMP with higher affinity than 2'3'-cGAMP. It was, however, selective for 2'3'-cGAMP relative to the small molecules ATP and GTP. Ultimately, the biosensor was used to

quantify 2'3'-cGAMP production in mammalian cell lysates, with the estimated limit of detection in the assay being .95 μM, and calculated production to be on average 36 million molecules of 2'3'-cGAMP per activated cell.

Antibody generation

This project focuses on developing a sensitive and specific antibody to 2'3'-cGAMP, and the following is a review of general considerations and methods for antibody generation.

History and background of monoclonal antibody generation

The history of antibody generation begins with the first reference to anti-sera and antibodies in 1890 by Emil von Behring and Shibasabura Kitasato (work for which von Behring was awarded the 1901 Nobel Prize in Physiology or Medicine) (Llewelyn, Hawkins, & Russell, 1992). Soon after, Paul Ehrlich, a pioneering scientist (and Nobel Laureate) in immunology and medicine, proposed a general model for antibodies and their antigen recognition. The 1950s was marked by a series of crucial discoveries in the field, including identification of plasma B cells as antibody generators, the first molecular structure of an antibody, and the idea of clonal selection. In 1975, Georges Köhler and César Milstein, generated the first mouse monoclonal antibodies *in vitro* (for which they were awarded the 1984 Nobel Prize in Physiology or Medicine), ushering in an exciting era of antibody development and technologies (Kohler & Milstein, 1975). Procedures for design and creation of antigen-specific monoclonal antibodies are now well-established and widely used in laboratory settings.

The choice of animal species for antibody production depends on multiple factors, with each species having benefits and limitations (Leenaars & Hendriksen, 2005). Academic labs often utilize smaller animals like mice, rats, and rabbits; larger animals such as goats and sheep are often used as well, especially in industry settings. Mice are easy to obtain and handle,

require a shorter timeline for immunization, and (as explained below) monoclonal antibody generation can be performed in an academic laboratory setting. Furthermore, because mice are smaller, they require less antigen/hapten-carrier complex for immunization, which is beneficial when these reagents are limiting. However, the amount of antibody produced in mouse sera is small, and obtaining large amounts of sera is difficult. Additionally, mouse spleens are quite small and contains less cells than that of a rabbit, for example. Rabbits are a preferred choice for several reasons, most obvious being the larger sample volume and thus amount of antibody obtainable. In general, rabbit antibodies have higher affinities than that of mice, and can recognize human antigens that are typically non-immunogenic in mice (Landry, Ke, Yu, & Zhu, 2015; Rossi et al., 2005). Rabbits tend to be superior to other species for generating responses to small molecules and peptides, with less response towards the associated carrier proteins (Feng, Wang, & Jin, 2011). Rabbits also have an immune system unique to that of humans and mice, in that they use unique strategies for antibody repertoire diversification (Weber, Peng, & Rader, 2017). Finally, rabbit IgG also has no subclass, and its structure is simpler than that of mice and humans, making it more amenable to recombinant antibody production/cloning and engineering.

Successful immunization of an animal (commonly mouse or rabbit) with foreign antigen results in the production of polyclonal antibodies, each generated from a distinct B cell lineage and specific to a unique epitope on the antigen. Monoclonal antibodies, in contrast, are made by a single B cell (or identical clones of a parent B cell), and all bind the same epitope of the antigen. The technique developed by Kohler and Milstein allowed for mouse monoclonal antibody isolation through a process known as hybridoma generation. Hybridoma cells are the fusion product of splenic B-lymphocytes of an immunized mouse and an immortal myeloma (a type of plasma cell cancer) cell line lacking the hypoxanthine-guanine-phosphoribosyltransferase

(HGPRT) gene, a gene essential for nucleotide synthesis from the purine salvage pathway. Additionally, the myeloma cell line used does not produce any antibodies. Upon culture in selective medium containing hypoxanthine-aminopterin-thymidine, only successfully-fused hybridomas will survive: aminopterin inhibits nucleotide synthesis and thus unfused myeloma cells will die, and the individual mouse B-cells have a limited lifespan and will also die. Hybridoma cells retain the best characteristics of each cell type: they can produce a monoclonal antibody throughout their indefinite time in culture (Yokoyama et al., 2013).

Soon after the introduction of mouse monoclonal antibody isolation, there were several failed attempts to adapt the technique for rabbits. It proved extremely difficult to generate a stable myeloma cell line fusion partner, and it was not until the late 1990s that the first rabbit hybridoma was generated (Spieker-Polet, Sethupathi, Yam, & Knight, 1995). Over the last few decades the fusion partner has been subcloned and selected, but the process of rabbit hybridoma generation is still considered extremely difficult and alternative methods are often used (Liguori, Hoff-Velk, & Ostrow, 2001).

As mentioned above, isolated splenic antibody-producing B-cells have a relatively short lifespan *in vitro*. However, recent advances in culture techniques have allowed companies and some labs to extend their lifespan long enough to screen clones for positive antibodies, and isolate RNA for sequencing and subsequent recombinant antibody generation (Ettinger et al., 2005).

Small molecule antibody generation

Although techniques for animal immunization are relatively straightforward when the antigen of interest is a protein, small molecule antibody generation often proves difficult. Short peptides or small compounds are generally too small (especially with molecular weights less

than 1000) and lack the complexity to be recognized by the immune system, or to be processed in a way that elicits an immune response – they are non-immunogenic. This issue is circumvented by conjugation of the small molecule, or hapten, to an immunogenic carrier protein; when an animal generates an immune response to the hapten-carrier conjugate, antibodies are produced to epitopes on both the small molecule and the carrier protein (Rajewsky, Schirrmacher, Nase, & Jerne, 1969). With subsequent screening and selection, one can easily isolate antibodies specific to the small molecule.

The most widely used carrier proteins include Keyhole Limpet Hemocyanin isolated from the limpet *Megathura crenulata* (mcKLH), and Bovine Serum Albumin (BSA). mcKLH is a very large and complex molecule, composed of subunits with a molecular weight of approximately 390,000 Daltons that assemble into decamers or didecamers. BSA is a much smaller, but still immunogenic carrier, with a weight of 67 kilodaltons (Singh, Kaur, Varshney, Raje, & Suri, 2004).

There are several ways to join a hapten to carrier proteins, largely dependent on the functional groups available on both molecules for conjugation (Hermanson, 2013). It is also important to consider the location of functional groups and anticipate the overall structure of the resulting carrier-hapten complex – certain areas of the hapten may be 'hidden' or obstructed from view of the immune system. Because mcKLH and BSA both have many surface lysines exposed, primary amines are often targeted for conjugation. Alternatively, exposed cysteine residues with free sulfhydryl groups, as well as carboxylic groups from aspartate and glutamate may be targeted. Free amines and carboxyl groups can be crosslinked using EDC chemistry: EDC is a carbodiimide crosslinker that reacts with a free carboxylic acid on either the carrier or hapten to generate a labile intermediate, which can react with a free primary amine on the

remaining molecule (carrier or hapten, depending) to form a covalent amide bond between the hapten and carrier. Free sulfhydryl (thiol) groups will react readily with maleimide functional groups at a pH of 6.7 to 7.5 to form a thioether bond. Both mcKLH and BSA can be purchased in an activated form containing maleimide function groups at every available primary amine (lysine) (Singh et al., 2004).

Another crosslinking method gaining popularity is click chemistry. The nature and mechanism of this technique was first described in 2001 by Nobel Laureate (in chemistry) K Barry Sharpless (Kolb, Finn, & Sharpless, 2001). The reaction entails coupling an azide and alkyne through a copper-catalyzed reaction, yielding a covalent product: 1,5-disubstituted 1,2,3-triazole. It has become a widely-used technique *in vitro* and now *in vivo* for several reasons: firstly, the azide and alkyne reactant pairs are unique to nature, and although they are mutually reactive, they do not cross-react or interact in a major way with other biological molecules, so formation of side products is not concern. The cycloaddition reaction is thermodynamically favorable, so the reaction proceeds quickly and is very specific, and the resulting product is quite stable. Lastly, it can be performed in a wide variety of conditions, and is pH insensitive (Mackinnon & Taunton, 2009).

Goal of current research

The recent appreciation for the involvement of cGAS-cGAMP-STING signaling in numerous clinical phenotypes necessitates development of tools that can outline the true extent of its contribution to various diseases, and in patients with aberrant pathway activity, to provide a rationale for targeted therapy. Additionally, numerous questions remain regarding the details and regulation of cGAS-cGAMP signaling. We need to better understand the pathway's regulation and termination, and specifically understand the dynamics of 2'3'-cGAMP signaling, localization, and clearance within the cGAS-STING pathway. We also desire a tool to explore the potential role of 2'3'-cGAMP in other systems outside of innate immunity.

My work focuses on the development of an antibody of high sensitivity and specificity for this small molecule second messenger, capable of recognizing and quantifying 2'3'-cGAMP production *in vivo*. Herein we describe the generation of a hapten-carrier antigen that allows for successful immunization of animals against 2'3'-cGAMP, and subsequent isolation of unique monoclonal antibodies. We perform a detailed characterization of the biochemical properties of one of these antibodies, to better understand its sensitivity and specificity, *in vitro* and *in vivo*. We adapt it for use in a wide variety of techniques: to track and measure levels of 2'3'-cGAMP quantitatively, to visualize 2'3'-cGAMP produced in cells, and to quickly identify cGAMP-positive cell populations within live samples. We show this antibody to be an invaluable tool to elucidate outstanding questions in the field, and demonstrate its potential to detect patients with aberrant activation of the cGAS-STING pathway.

CHAPTER TWO
RESULTS

Generation of mouse antibodies to 2'3'- cGAMP – successes and failures

As mentioned above, there are several ways to conjugate a hapten to an immunogenic carrier protein. Initially, our efforts aimed at generating a monoclonal mouse antibody against 2'3'-GAMP by using hybridoma technology. Multiple 2'3'-cGAMP analogs were synthesized by collaborators from the laboratory of Dr. Chuo Chen, specifically postdoctoral fellow Dr. Heping Shi – these varied in the functional groups available for conjugation to mcKLH and BSA, and are shown in Figure 3.

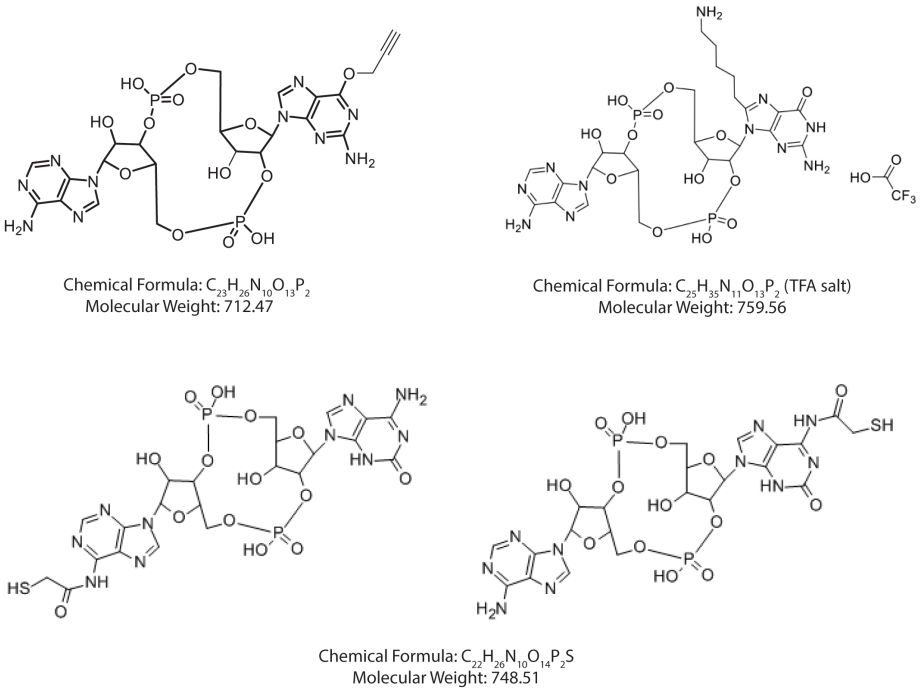

Figure 3. Modified Forms of 2'3'-cGAMP Used for Immunization.
Compounds were synthesized by Dr. Heping Shi, from the lab of Dr. Chuo Chen, in the Chemistry Department of UT Southwestern.

An initial attempt was made using an analog of 2’3’-cGAMP containing a thiol residue, for conjugation to maleimide-activated mcKLH. Although immunized mice produced a polyclonal antibody response to the carrier protein (the carrier protein and the maleimide linker), no response to 2’3’-cGAMP was detected despite attempts in over 16 mice.

A second attempt involved an amino group-modified 2’3’-cGAMP, with the primary amine extending from 2’3’-cGAMP on a long carbon chain. EDC crosslinking was used for conjugation, and the formation of the complex was monitored indirectly using Mass Spectrometry (MS) to measure a decrease in the starting material 2’3’-cGAMP over time. Unfortunately, despite multiple attempts at condition optimization, consumption of the amino-2’3’-cGAMP was never observed with MS.

A third and final attempt to generate a cGAMP-KLH or cGAMP-BSA complex utilized click chemistry. The 2’3’-cGAMP analog used contained an alkyne group, and was synthesized by Dr. Heping Shi – this synthesis will be described elsewhere. First, KLH and BSA were modified with azide groups at any available primary amines, using the compound NHS-Peg4-Azide. The azide functional group that remains after attachment to amine residues has a molecular weight of approximately 274.29 g/mol, and because BSA and KLH have many available lysines for conjugation, their molecular weight will increase substantially upon azide addition. Thus, formation of the azide-modified carrier protein was readily monitored as a shift upward on a Coomassie-stained protein gel relative to the starting material carrier protein. The actual click chemistry step was then performed using the azide-modified carrier protein and the alkyne-modified 2’3’-cGAMP. Again, the complex formation was monitored as a shift upward on a Coomassie-stained protein gel of the reaction product relative to the starting material azide-carrier protein. As a second measure of successful conjugation, Mass Spectrometry was used to

monitor the consumption of the alkyne-modified starting material. Only a reaction mixture containing both the alkyne, the azide-carrier, and the copper-containing catalyst showed a decrease or disappearance of the alkyne-2'3'-cGAMP starting material (Figure 4).

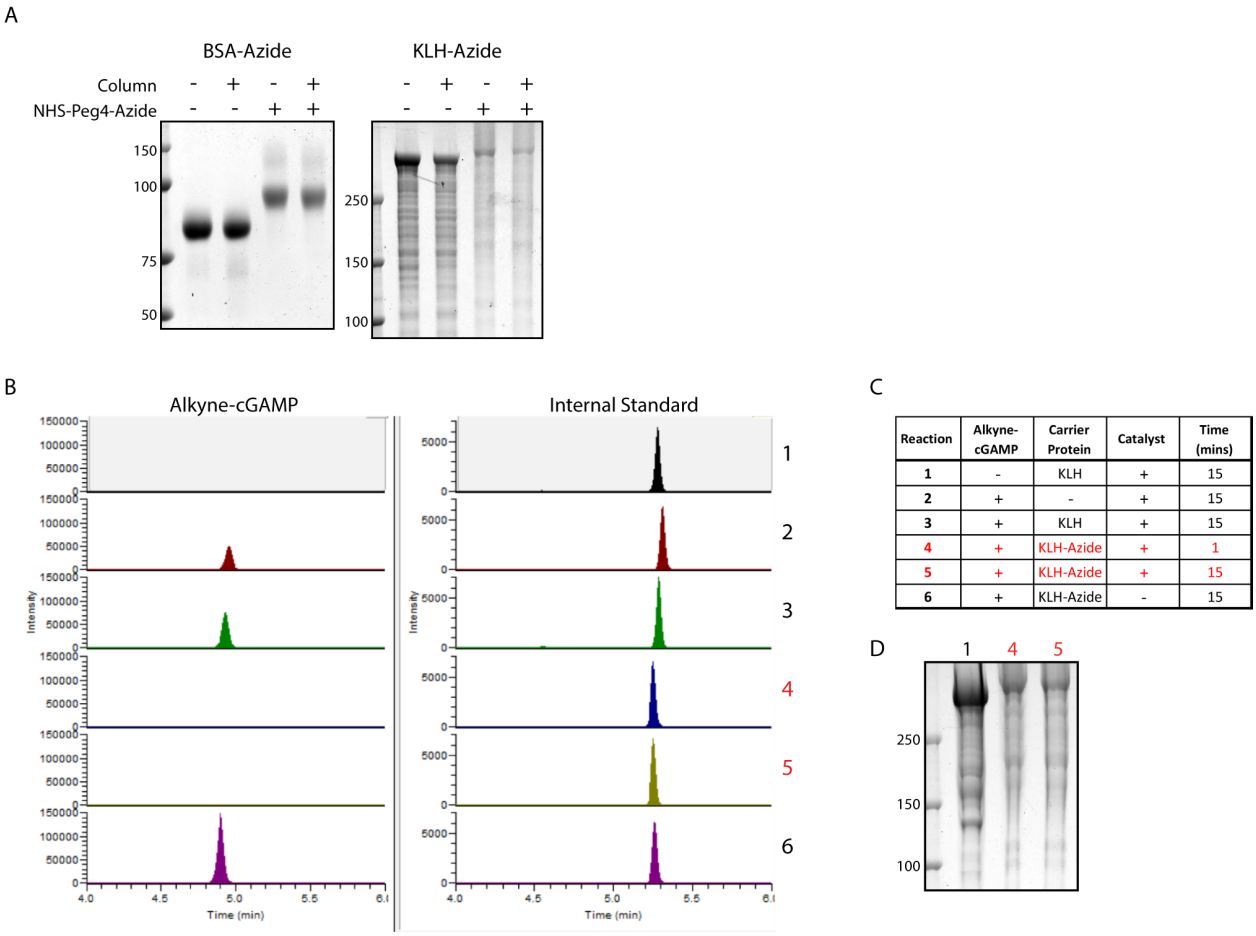

Reaction	Alkyne-cGAMP	Carrier Protein	Catalyst	Time (mins)
1	-	KLH	+	15
2	+	-	+	15
3	+	KLH	+	15
4	+	KLH-Azide	+	1
5	+	KLH-Azide	+	15
6	+	KLH-Azide	-	15

Figure 4. Synthesis of cGAMP-Carrier Protein Complex.
(A) Coomassie stained protein gels to monitor addition of azide functional groups to the indicated carrier protein, as indicated by a shift upward relative to unmodified carrier protein. 'Column' indicates purification of sample using a Zeba Spin Desalting Column. (B) Monitoring consumption of alkyne-cGAMP during click chemistry reaction, as measured by Mass Spectrometry. Left column shows the relative alkyne-cGAMP level, and right column shows the relative level of internal standard spiked into each sample. (C) Table indicating components of each click chemistry reaction monitored in (B). (D) Coomassie stained protein gel to monitor cGAMP-carrier protein complex formation, as indicated by a shift upward relative to unmodified carrier protein.

With a stable cGAMP-carrier protein conjugate in hand, we immunized four WT BALB/c mice over the course of weeks, periodically testing sera for antibody production. All four immunized mice showed an antibody response to 2'3'-cGAMP, as well as the carrier protein and linker region, although to varying degrees.

To further characterize the sensitivity and specificity of the antibody response, we established a competitive ELISA assay, in which a biotinylated form of 2'3'-cGAMP is conjugated to a streptavidin-coated ELISA plate (Figure 5). A pre-incubated solution of antibody and varying concentrations of free 2'3'-cGAMP are added to the plate, and after secondary antibody treatment, any antibody not bound to the coated plate will be removed through washing steps. Increasing the concentration of free 2'3'-cGAMP incubated with sera (or purified antibody) should result in a decreased final signal (OD 450 value). As shown in Figure 6a and 6b, this indeed was the case for the mouse polyclonal sera. As a preliminary assessment of antibody specificity, we also incubated the mouse sera with varying concentrations of other small molecules, and no competition was observed (Figure 6a,b).

We next attempted to isolate monoclonal antibodies to 2'3'-cGAMP using hybridoma technology. Two mice were chosen for splenic B cell isolation and hybridoma production, and approximately 1000 clones were generated from each fusion. These clones were screened for a positive response on the biotin-cGAMP coated ELISA, and approximately 34 were selected for further expansion and testing. The 34 clones were tested for binding to 2'3-cGAMP, as well as the KLH carrier protein and the linker between the carrier protein and 2'3'-cGAMP – only four were completely specific to 2'3'-cGAMP and not the carrier protein or linker region. However, none of these four antibodies showed a response on the competitive ELISA, even after purification with a Protein G column.

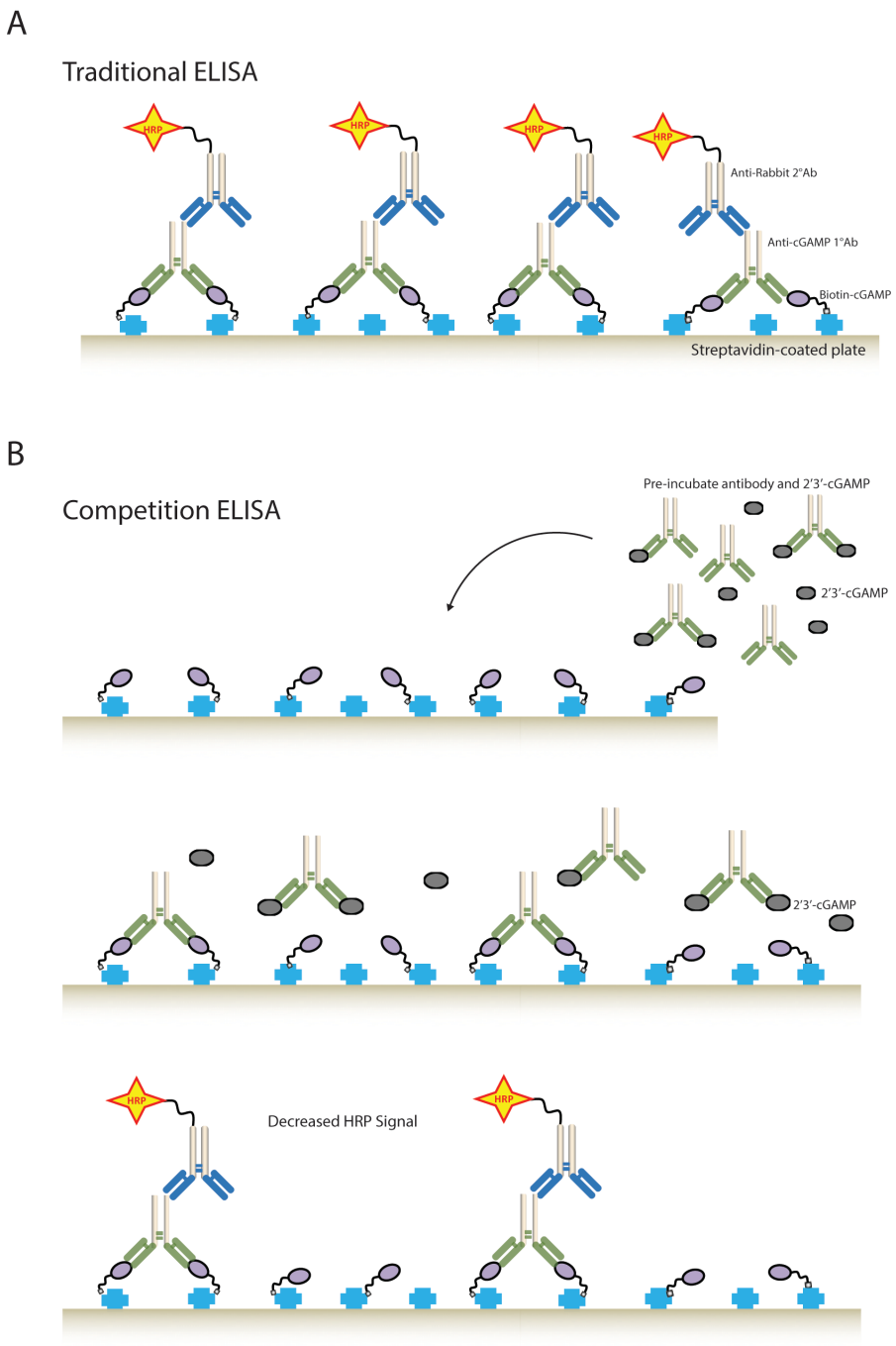

Figure 5. Schematic of ELISAs to Characterize 2'3'-cGAMP Producing Antibodies.
(A) Standard ELISA assay: Biotinylated 2'3'-cGAMP is conjugated to a streptavidin-coated ELISA plate, followed by incubation directly with animal sera (serves as the primary antibody). Subsequent incubation with HRP-linked secondary antibody followed by standard developing procedures will lead to a measurable color change (OD 450 value). (B) Competitive ELISA assay: A pre-incubated solution of antibody/sera and varying concentrations of free 2'3'-cGAMP (or other small molecule) are added to the biotin-cGAMP conjugated plate, and after HRP-linked secondary antibody treatment, any primary antibody not bound to the coated plate will be removed through washing steps. Increasing the concentration of free 2'3'-cGAMP incubated with sera/antibody should result in a decreased final signal (OD 450 value). Figure generated in Adobe Illustrator, 6th edition.

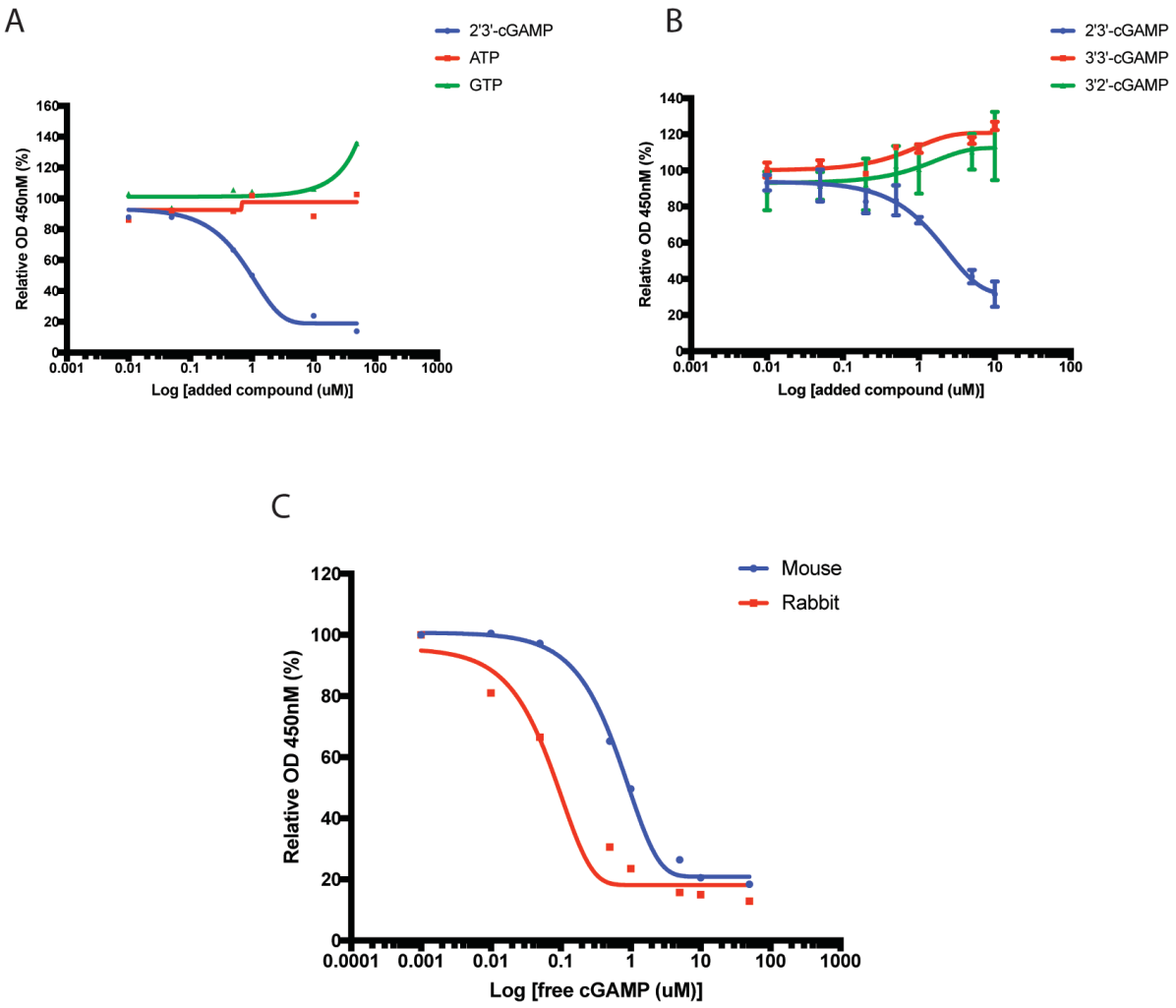

Figure 6. Immunized Mice and Rabbits Produce a Polyclonal Response to 2'3'-cGAMP. Sensitivity and specificity of mouse and rabbit sera as determined by competitive ELISA assays. (A) Sera from Mouse #1 was pre-incubated with increasing concentrations of 2'3'-cGAMP, ATP, or GTP. (B) Sera from Mouse #1 was pre-incubated with increasing concentrations of 2'3'-cGAMP, 3'2'-cGAMP, or 3'3'-cGAMP. (C) Mouse or rabbit sera was pre-incubated with increasing concentrations of 2'3'-cGAMP. All ELISAs were performed as indicated in Methods section. Curves were generated using GraphPad Prism 5.0 software. Error bars indicate standard deviation of duplicate measurements.

Generation of rabbit antibodies to 2'3'-cGAMP – polyclonal and monoclonal

We next moved to immunization in rabbits, for reasons mentioned in the introduction. Rabbits are immunized in an analogous fashion to mice, although the overall time frame is longer, and amounts of injected material differ. It should also be noted that when using a hapten, the carrier protein used for immunization is switched after the first few immunizations (in our case, initial injections were performed with cGAMP-KLH, followed by injections with cGAMP-BSA). As shown in Figure 6c, an appropriate polyclonal response was generated against 2'3'-cGAMP (and the carrier protein), and binding to the biotin-cGAMP ELISA plate could be successfully competed out by adding free 2'3'-cGAMP. Ultimately, peripheral blood mononuclear cells (PBMCs) were harvested from rabbit blood (the rabbit does not need to be sacrificed for this), and B-cells were separated and individually cultured long enough to collect a small amount of secreted antibody. Over 700 B-cells were cultured and screened for their ability to produce antibodies to 2'3'-cGAMP; 123 of these cells generated a positive response. These 123 were subsequently tested in the competitive ELISA, and although many had some degree of response, we chose to follow up on the 20 highest responders. Through collaboration with Dr. Zhiqiang An at the University of Texas at Houston, we isolated RNA from these 20 B-cells and cloned the antibody genes – this revealed that there were actually a total of 36 heavy chains and 33 light chains, leading to a total of 61 possible heavy/light chain combinations. These results suggest that some of the B cell cultures were not derived from a single clone. These 61 recombinant antibodies were cloned into expression vectors and used for small-scale transfections to obtain secreted recombinant antibody, which were subsequently tested via competition ELISA for a response. We chose to further characterize several of these antibodies, and below is a comprehensive study of one of these top performers.

Recombinant monoclonal antibodies to 2'3'-cGAMP have extremely high sensitivity

Ultimately, we obtained several purified clones capable of recognizing 2'3'-cGAMP with high affinity, with binding constants in the low nanomolar range (Figure 7). We chose one antibody for further characterization, and found it had a K_d value of approximately 10.88 nM, a K_{on} of 2.922×10^5 $M^{-1}s^{-1}$, and a K_{off} of $3.180 \times 10^{-3} s^{-1}$. Previous studies from our lab establish the binding between 2'3'-cGAMP and the adaptor protein STING to be of similar affinity (~4 nM).

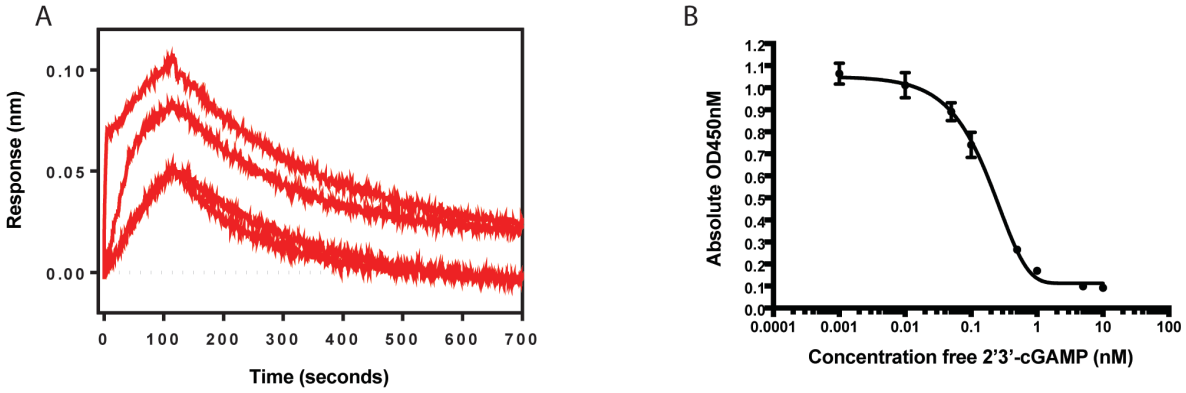

Figure 7. Sensitivity of Antibody:2'3'-cGAMP Interaction.
(A) Sensorgram generated by collaborator (Dr. Mark Gui). Values of calculated kinetic parameters (K_d, K_{on}, K_{off}) from graph can be found within main text. (B) Sensitivity of antibody as determined by competitive ELISA assay. Antibody was pre-incubated with increasing concentrations of 2'3'-cGAMP from .001 to 10 nM, and added to a biotin-cGAMP coated ELISA plate. ELISA was performed as indicated in Methods section. Curve was generated using GraphPad Prism 5.0 software. Error bars indicate standard deviation of triplicate measurements.

Rabbit monoclonal antibody shows a high degree of specificity for 2'3'-cGAMP

We next characterized the ability of our antibody to discriminate between 2'3'-cGAMP and other similarly structured small molecules. The nucleotides used by cGAS to produce 2'3'-cGAMP - ATP and GTP - are readily available within cells, necessitating the use of an antibody extremely specific for the unique structure of 2'3'-cGAMP. As measured by competitive ELISA described above, our antibody was not capable of recognizing ATP, GTP, or their respective

precursors. These small molecules could not compete for antibody binding, even at micromolar concentrations (Figure 8a).

Although 2’3’-cGAMP is the only cyclic dinucleotide produced in metazoans, a variety of bacteria utilize the cyclic dinucleotides cyclic-di-GMP and cyclic-di-AMP for signal transduction. As shown in (Figure 8a), although the overall structure of these second messengers resembles that of 2’3’-cGAMP, our antibody does not recognize these molecules to any measurable degree.

As previously elucidated by our lab, cGAMP contains two phosphodiester bonds connecting the GMP and AMP components. This allows for a total of four possible cGAMP isomers, differing only in their internal phosphodiester linkages. Although 2’3’-cGAMP is the only isomer produced by endogenous cGAS, all isomers are capable of binding to STING, and all can potently induce IFN-β. Using the competitive ELISA assay, we tested the specificity of our antibody to each of these isomers, and found the antibody to be highly specific for 2’3’-

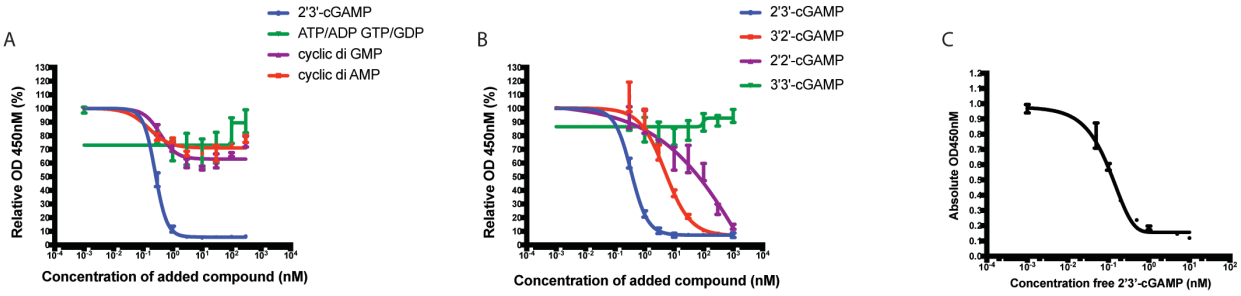

Figure 8. Characterization of Antibody Specificity for 2’3’-cGAMP.
(A) Antibody was incubated with increasing concentrations (.001 to 1000 nM) of 2’3’-cGAMP, cyclic di GMP, cyclic di AMP, or a mixture of equal amounts of ATP, ADP, GTP and GDP. (B) Antibody was incubated with increasing concentrations (.001 to 1000 nM) of possible cGAMP isomers: 2’3’-cGAMP, 3’2’-cGAMP, 2’2’-cGAMP, or 3’3’-cGAMP. (C) Increasing concentrations of 2’3’-cGAMP (from .001 to 10 nM) were spiked in to heat sup collected from unstimulated THP-1 cells, and the mixture was incubated with antibody.
All ELISAs were performed as indicated in Methods section. Curves were generated using GraphPad Prism 5.0 software. Error bars indicate standard deviation of triplicate measurements.

cGAMP. Only at high concentrations was a small degree of competition by 3'2'-cGAMP noted, and by 2'2'-cGAMP at even higher concentrations. 3'3'-cGAMP was not able to compete for binding to the antibody in our assays. These results are quite remarkable, considering the high degree of similarity between these isomers, and demonstrate the excellent specificity of our antibody for 2'3'-cGAMP (Figure 8b).

Antibody can detect 2'3'-cGAMP produced in cells stimulated with DNA

We next sought to determine whether the antibody could recognize 2'3'-cGAMP in the context of a complex cellular environment. Importantly, the antibody must be able to detect 2'3'-cGAMP produced by cellular cGAS upon pathway stimulation. Human monocytes (THP-1 cell line) were stimulated with herring testis DNA (HT-DNA) for varying lengths of time, followed by cell lysis and boiling to denature any proteins. The resulting supernatant (referred to here as 'heat sup') was tested for the presence of 2'3'-cGAMP using the competitive ELISA assay, and a reference standard curve was also generated by spiking in known amounts of 2'3'-cGAMP into unstimulated THP-1 heat sup (Figure 8c). As shown in Figure 9c, cells activated by HT-DNA produce steadily increasing levels of 2'3'-cGAMP, mirroring the increase in phosphorylation (activation) of downstream pathway components IRF3 and TBK-1 (Figure 9a), as well as the rise of IFN-β induction (Figure 9b). As a control, the amount of 2'3'-cGAMP estimated in each sample was similar to that measured using quantitative mass spectrometry (Figure 9c). Thus, measurement of 2'3'-cGAMP production with our antibody serves as a reliable method to monitor cGAS-STING signaling in DNA-stimulated cells.

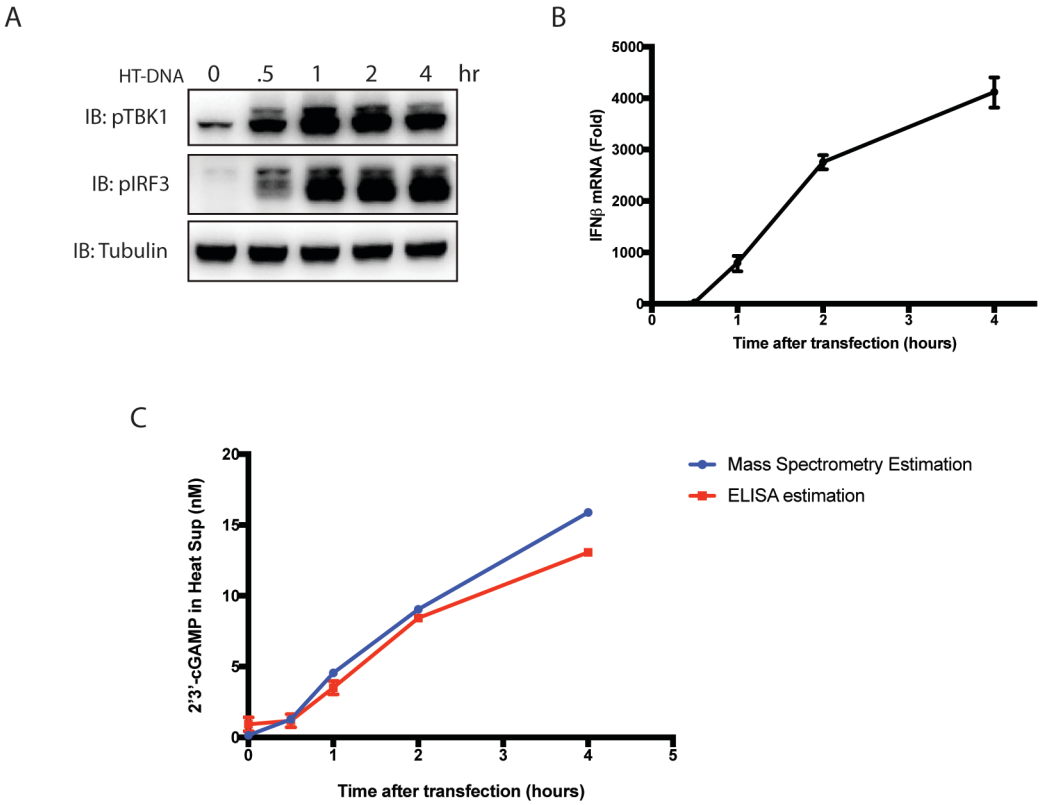

Figure 9. Antibody Detects 2'3'-cGAMP Produced in DNA-Stimulated Cells.
WT THP-1 cells were stimulated with 2μg/mL HT-DNA for indicated time intervals, and each sample was divided into four groups for subsequent analysis: (A) immunoblotting of cell lysate for phosphorylation of TBK1 and IRF3 (B) qRT-PCR analysis of relative IFN-β expression (C) quantification of 2'3'-cGAMP levels in heat sup using competitive ELISA assay or Mass Spectrometry. All curves were generated using GraphPad Prism 5.0 software. Error bars indicate standard deviation of triplicate measurements.

Antibody can detect 2'3'-cGAMP produced in cells stimulated with virus

An analogous experiment was performed by infecting cells with a mutant strain of Herpes Simplex Virus (here referred to as HSVΔ34.5). Like the HT-DNA transfected cells, virally infected cells were found to contain increased levels of 2'3'-cGAMP over time. (Figure 10b). Again, we monitored pathway activity using well-accepted methods, namely phosphorylation of TBK1 and IRF3 (Figure 10a). This experiment, along with the DNA stimulation experiment, demonstrate the ability of our antibody to specifically recognize 2'3'-cGAMP from a multitude of cellular contents.

A

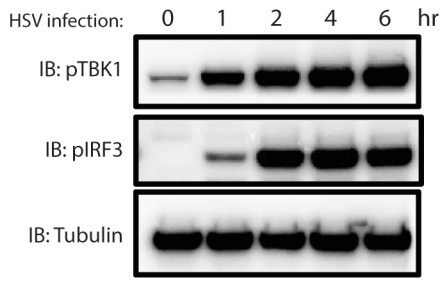

B

HSV Infection			
Infection time	Average OD450	Std. dev	Est. cGAMP (nM)
0h	**1.126**	0.082	
1h	**1.027**	0.05	0.026
2h	**0.77**	0.078	0.152
4h	**0.599**	0.056	0.268
6h	**0.702**	0.105	0.194

Figure 10. Antibody Detects 2'3'-cGAMP Produced in Virally Infected Cells.
WT THP-1 cells were stimulated with HSVΔ34.5 at an MOI of 10 for indicated time intervals, and each sample was divided into four groups for subsequent analysis: (A) immunoblotting of cell lysate for phosphorylation of TBK1 and IRF3 (B) quantification of 2'3'-cGAMP levels in heat sup using competitive ELISA assay. All curves were generated using GraphPad Prism 5.0 software. Error bars indicate standard deviation of triplicate measurements.

Antibody can be used to visualize 2'3'-cGAMP produced within stimulated cells

Next, we tested ability of the antibody to determine the cellular localization of endogenous 2'3'-cGAMP using confocal immunofluorescence microscopy. Human epithelial cells (BJ cell line) stably expressing a Flag-tagged STING adaptor protein were treated with HT-DNA, and stained with the 2'3'-cGAMP antibody. Only cells with successful pathway activation, as demonstrated by STING perinuclear puncta formation, stained positive for 2'3'-cGAMP (Figure 11a). The 2'3'-cGAMP signal was diffuse throughout the cytoplasm of activated cells. This was also shown to be the case in HSV-infected HeLa cells (Figure 11b). We noted a change in cell appearance after HSV infection, which was expected based on previous studies that observe a change in cell morphology with infection. Both stimulation conditions were successfully repeated in a variety of additional cell types, including murine embryonic fibroblasts and L929 cells (data not shown).

Antibody can be used to visualize 2'3'-cGAMP-producing cell populations with cell sorting

As a complementary method to identify 2'3'-cGAMP-containing cells, we tested the antibody's utility in cell sorting experiments. WT Murine Embryonic Fibroblasts (MEFs) were treated with HT-DNA for varying time points, followed by staining and sorting with the 2'3'-cGAMP antibody. A clear population of 2'3-cGAMP positive cells formed upon treatment for 2 hours with HT-DNA, and the population size grew upon treatment for 4 hours. (Figure 12a). Mock-treated cells did not show any significant 2'3'-cGAMP staining. Using the confocal component of ImageStream, images were taken of individual 2'3'-cGAMP positive cells – these cells showed a diffuse cytoplasmic localization of the molecule, similar to that seen using traditional immunofluorescence.

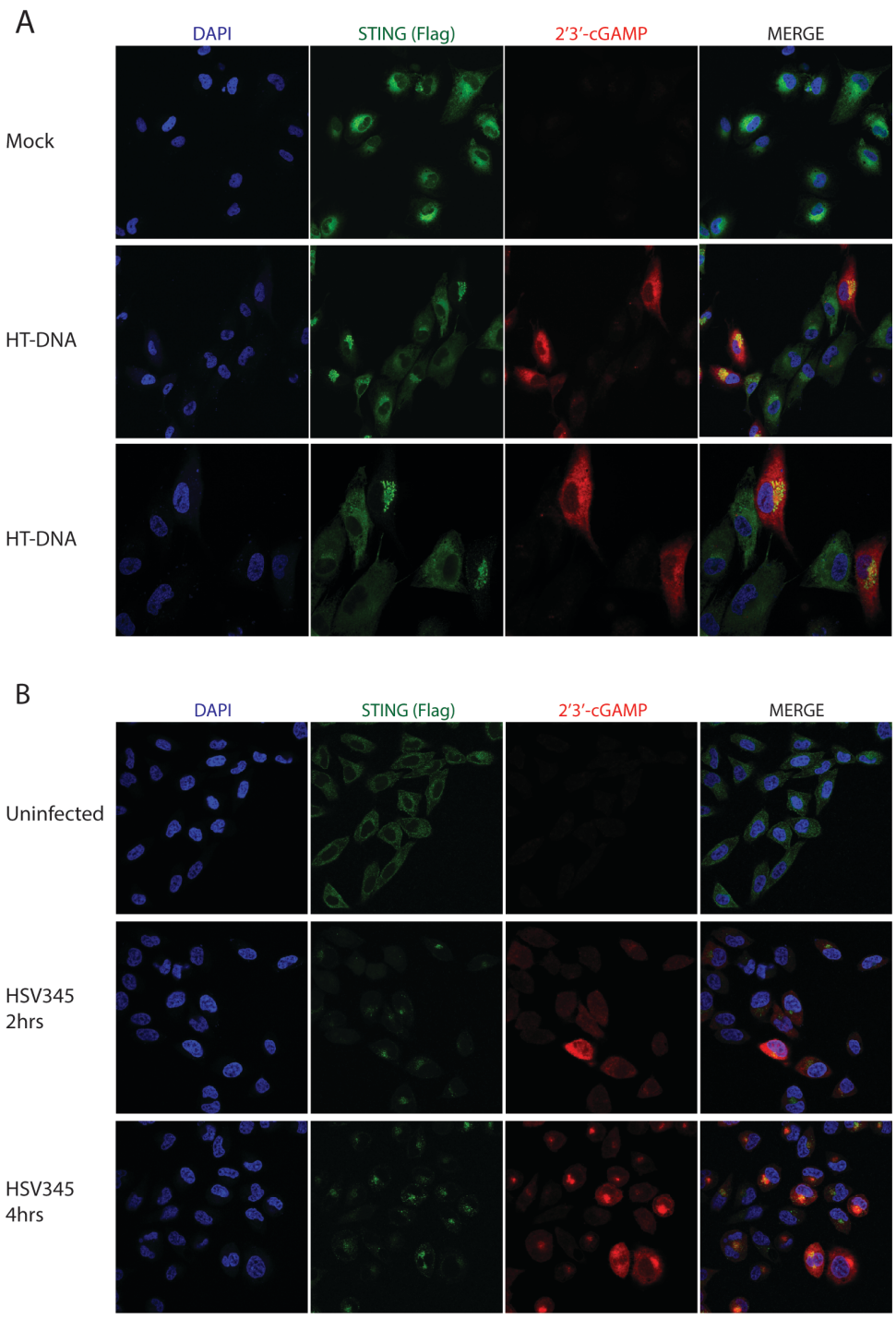

Figure 11. Antibody Visualizes 2'3'-cGAMP within Stimulated Cells.
(A) BJ STING$^{-/-}$ cells stably expressing Flag-tagged human STING were transfected with 2 μg/mL HT-DNA for 2 hours, and stained with DAPI along with Flag and 2'3'-cGAMP antibodies, followed by confocal microscopy. (B) WT Hela cells stably expressing Flag-tagged human STING were infected with HSVΔ34.5 at an MOI of 10 for indicated time intervals, and stained with DAPI along with Flag and 2'3'-cGAMP antibodies, followed by confocal microscopy.

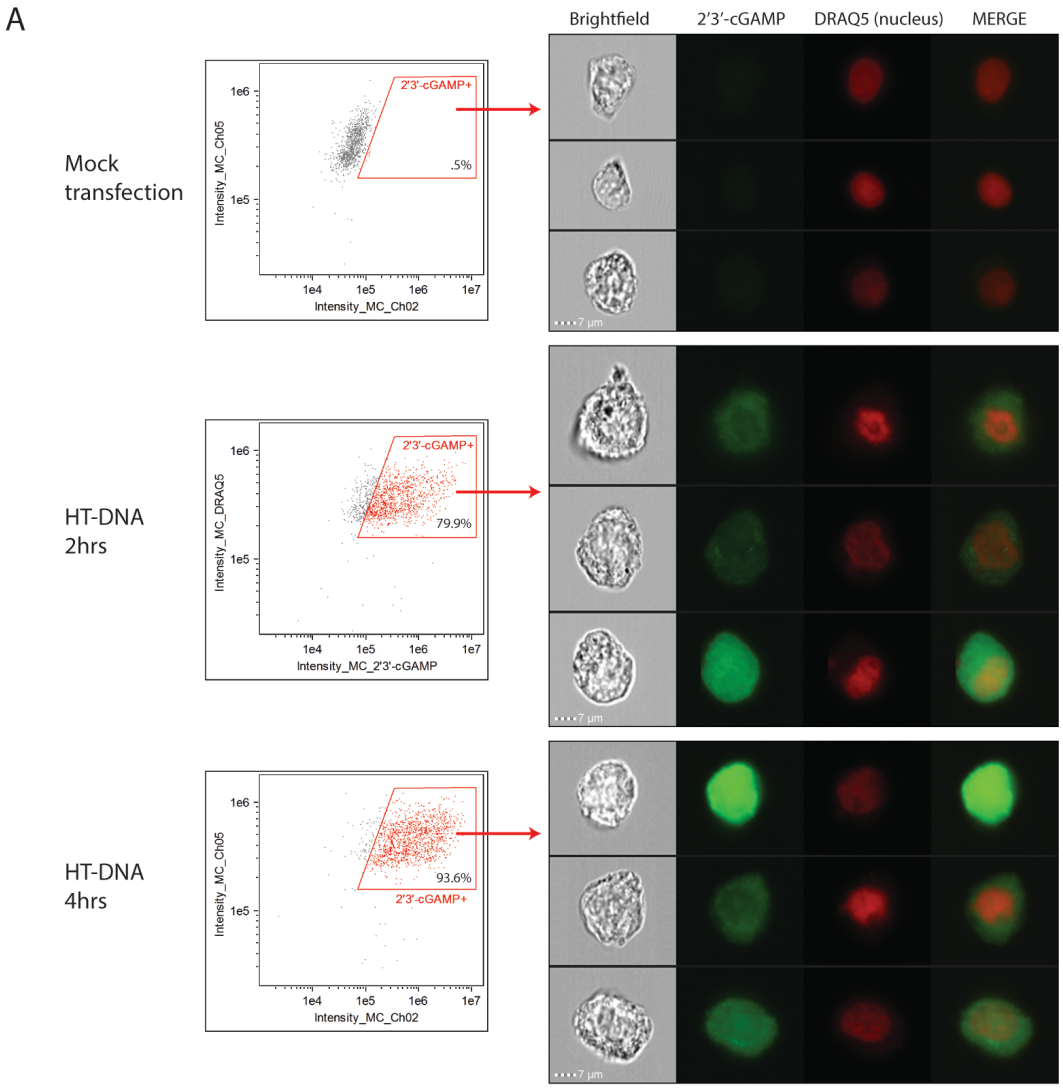

Figure 12. Antibody Can Recognize 2'3'-cGAMP Producing Cell Populations.
(A) WT Murine Embryonic Fibroblasts (MEFs) were treated with 2µg/mL HT-DNA for indicated time points followed by fixation, permeabilization, and staining with 2'3'-cGAMP antibody and DRAQ5. Single cell images were acquired using an ImageStream instrument, and analyzed by IDEAS software.

Additionally, we transiently overexpressed human cGAS tagged with GFP into Hela cells deficient in cGAS. Immunostaining with the 2’3’-cGAMP antibody verified the ability of transfected cGAS-GFP to produce 2’3’-cGAMP, and only cells containing cGAS-GFP could produce 2’3’-cGAMP (Figure 13a). When cells were subject to FACS analysis, this distinct population of cells that both express cGAS-GFP and produce 2’3’-cGAMP were easily observed (Figure 13b). These samples were stained with DRAQ5 and analyzed using Imagestream technology. After gating out live and in-focus cells, we identified two distinct populations of cells based on cGAS-GFP expression: either ‘cGAS positive’ or ‘cGAS negative cells’ (Figure 14). Of the cells expressing high levels of cGAS-GFP, 75.4% were found to produce 2’3’-cGAMP (representative images show in Figure 13c and Figure 14). These cells showed a diffuse cytoplasmic localization of 2’3’-cGAMP, as well as puncta representing activated cGAS-GFP (puncta formation of cGAS upon pathway stimulation has been shown in previous studies) (L. Sun et al., 2013). However, using the same cutoff values to designate 2’3’-cGAMP-positivity, we found only 0.88% of the ‘cGAS negative’ population contained 2’3’-cGAMP; the single cell images of this population indicated that the 2’3’-cGAMP signal was much lower than the average signal produced by the 2’3’-cGAMP positive cells in the ‘cGAS positive’ population (Figure 14).

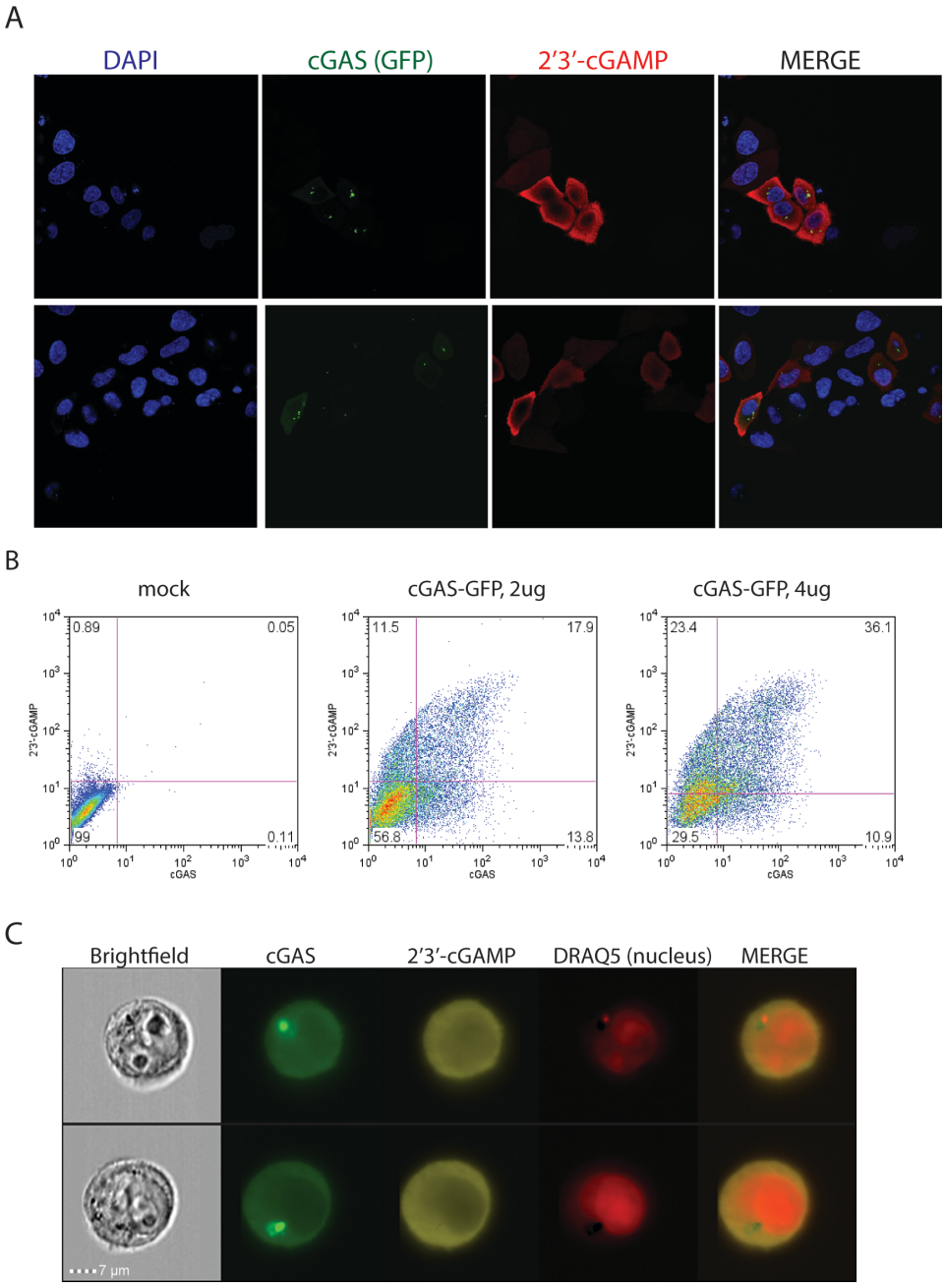

Figure 13. Antibody Can Visualize 2'3'-cGAMP Producing Cell Populations.
WT Hela cells were transiently transfected with GFP-tagged human cGAS for 24 hours. (A) Confocal microscopy images of cells stained with DAPI and 2'3'-cGAMP antibody (B) FACS analysis performed to assess the percentage of live cells both expressing cGAS and producing 2'3'-cGAMP (C) Representative images of single cells that both express cGAS and produce 2'3-cGAMP. Single cell images acquired with ImageStream instrument and analyzed by IDEAS software.

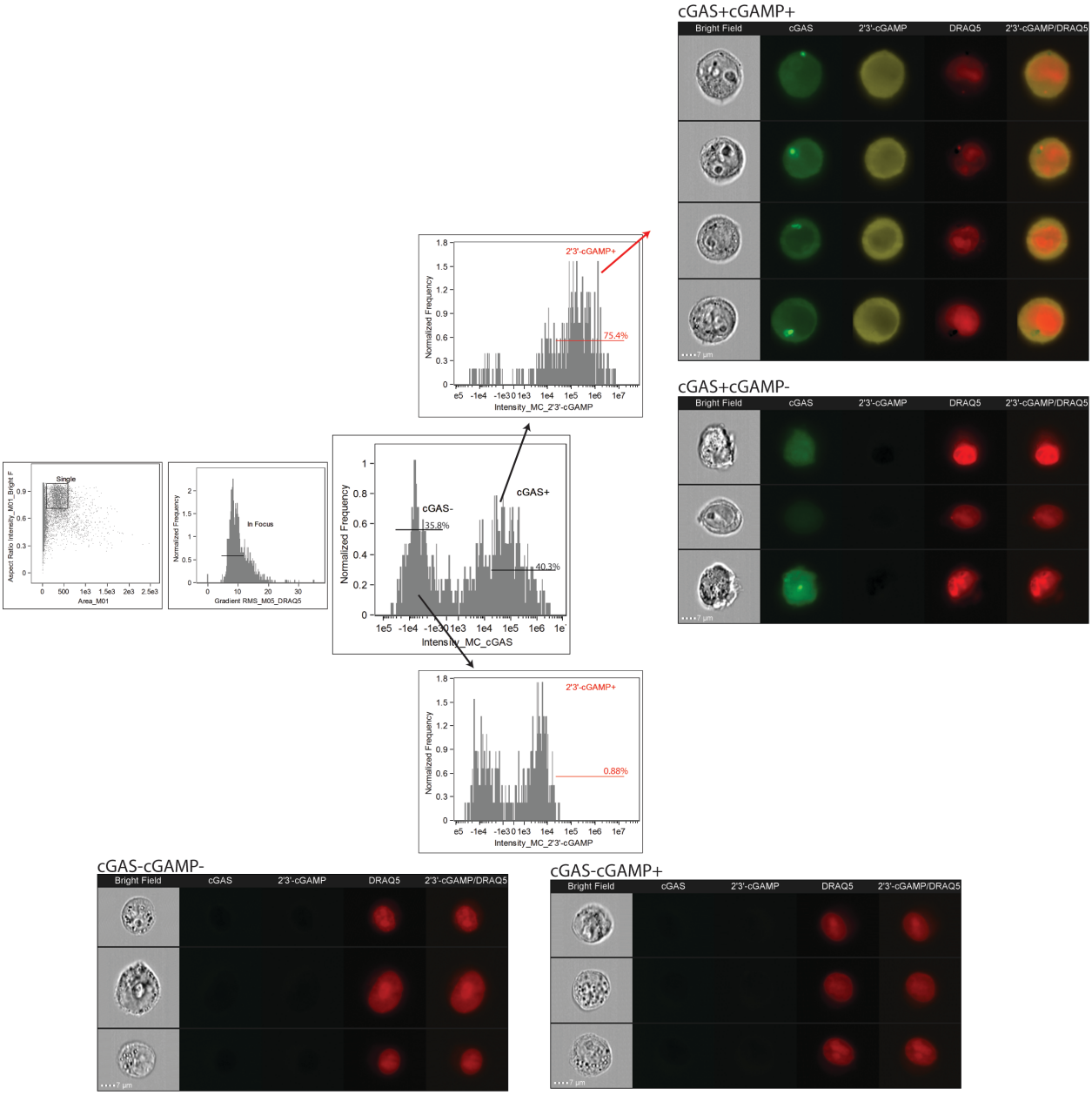

Figure 14. Gating Scheme and Control Cell Populations for Figure 13.
WT Hela cells were transiently transfected with GFP-tagged human cGAS for 24 hours, followed by staining with 2'3'-cGAMP antibody and DRAQ5, and processing with Imagestream technology. In-focus single cells were gated based on cGAS-GFP signal, and further gated based on 2'3'-cGAMP signal. Representative single cell images of each population are shown. Images of stained cells were acquired using an ImageStreamMarkII Flow Cytometer (Amnis), and acquired images were analyzed with Amnis software (IDEAS).

As mentioned in the introduction, a future goal of this project involves detection of 2'3'-cGAMP within autoimmune patient samples. Previous studies in the field have observed increased levels of 2'3'-cGAMP within patient PBMC samples – to confirm this finding, our antibody must be functional in PBMCs. We therefore isolated PBMCs from healthy human donor blood samples, and subsequently delivered 2'3'-cGAMP intracellularly by permeabilizing cells with perfringolysin O (PFO). Cells were then divided into two groups: as a control, the first group of cells was stained with antibody against human STING, because STING puncta formation is a hallmark of the cytosolic DNA sensing pathway's activation (Figure 15a). The second group of cells was stained with the 2'3'-cGAMP antibody, and 35.4% were shown to be positive for cGAMP production (Figure 15b). This was a smaller percentage than that of cells with STING puncta (77.1%).

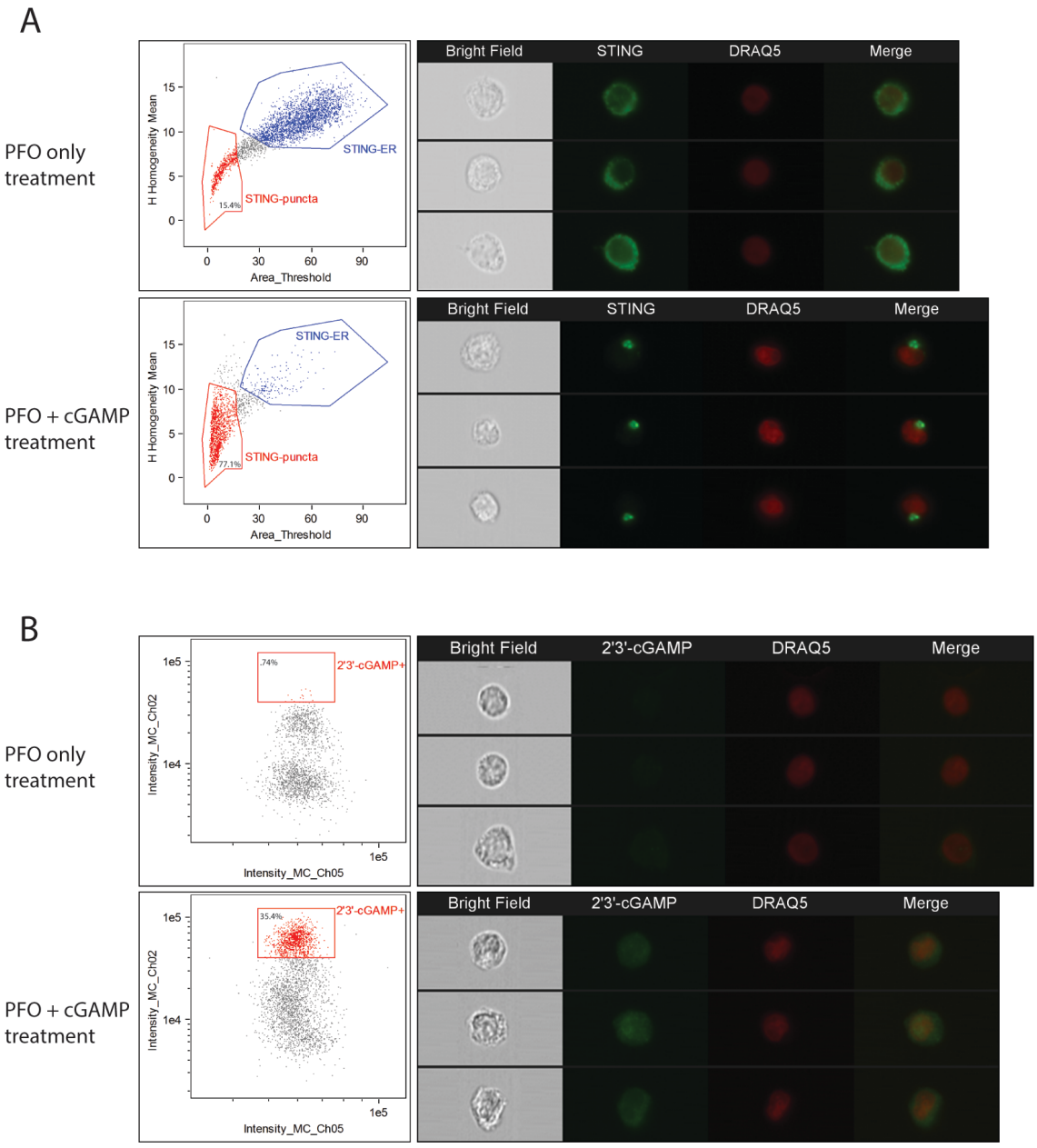

Figure 15. Antibody Can Detect 2'3'-cGAMP Introduced into Human PBMCs.
Human PBMCs were permeabilized with PFO and treated with 100nM 2'3'-cGAMP, followed by staining with DRAQ5 and (A) human STING antibody or (B) 2'3'-cGAMP antibody. Representative single cell images of each population are shown. Images of stained cells were acquired using an ImageStreamMarkII Flow Cytometer (Amnis), and acquired images were analyzed with Amnis software (IDEAS).

Conclusion of research project

In this study, we establish a reliable method for monitoring activity of the cGAS-STING pathway for cytosolic DNA sensing. We generated a rabbit monoclonal antibody capable of recognizing a hallmark of the pathway's activation, 2'3'-cGAMP production, with a high degree of sensitivity and specificity. This antibody readily distinguishes between 2'3'-cGAMP and other similarly structured small molecules normally found at high concentrations in cells. Its synthesis can be tracked and quantified in cells stimulated by exogenous DNA or pathogens, and its localization can be observed through imaging studies. 2'3'-cGAMP positive cell populations can be easily distinguished using flow cytometry methods. This antibody and methods that we developed will be useful tools to study the cGAS-STING pathway.

CHAPTER THREE
DISCUSSION

Challenges in generating monoclonal antibodies to 2'3'-cGAMP

Through collaboration with Dr. Heping Shi, we have synthesized and tested several strategies to conjugate 2'3'-cGAMP to carrier proteins. The first strategy involved reaction of a thiol-modified cGAMP to maleimide activated KLH, to form a covalent thioether linkage. There are multiple factors to consider when performing this reaction. First, maleimide groups specifically react with thiol moieties at a pH of 6.5-7.5 – thus, it is necessary to avoid higher pH conditions because of increased hydrolysis of the maleimide, as well as increased preference of the maleimide for amine functional groups. Secondly, although sulfhydryl groups of proteins are generally within disulfide bonds and will not react with maleimide, it is crucial to avoid any buffers containing thiol, such as beta-mercaptoethanol (BME) or dithiothreitol (DTT), because they can compete for reaction with maleimide. The exception, of course, is that thiol-containing buffers are needed when quenching any remaining maleimide upon reaction completion. Although errors in any of these requirements could have led to failure of the cGAMP-KLH conjugate, it is more likely an issue with the thiol-cGAMP analog itself. It is possible that the thiol groups are self-reactive and generate a disulfide bond between two molecules of cGAMP, making the sulfur groups inaccessible to the maleimide – essentially, the thiol-cGAMP may not be stable enough for performing the reaction, especially if it must be stored long-term before use. In an attempt to avoid this, we first treated the thiol-cGAMP with TCEP (tris(2-carboxyethyl)phosphine) – a reducing agent that does not react as readily with maleimide as BME and DTT. However, this may have been unsuccessful in either its reduction, or may have reacted with maleimide anyway. As mentioned in the results section, we attempted to immunize

multiple mice, and tried several conditions to optimize the reaction, but were never able to generate a response to 2'3'-cGAMP.

The second method attempted was reaction of an amine-containing cGAMP with an activated form of the carrier KLH, using what is known as EDC/NHS crosslinking chemistry to activate KLH. 1-Ethyl-3-(3-dimethylaminopropyl)carbodiimide (EDC) reacts at acidic pH conditions with available carboxylic acid residues to form an intermediate (known as an 'o-Acylisourea) which is very unstable. The stability is often improved by adding N-hydroxysuccinimide (NHS). The resulting NHS-ester intermediate can then react with primary amines to form a stable amide bond between the hapten and carrier protein. Main concerns include maintaining a low pH reaction, because hydrolysis of the NHS ester is increased with higher pH conditions, as well as avoiding buffers that contain primary amines which could compete for reaction. Although we tried to avoid these errors, we were not able to obtain a stable cGAMP-KLH conjugate.

At least for our purposes, click chemistry seemed superior to these techniques for many reasons, namely: the reaction is amenable to a wide variety of conditions and pH values, side products are not a concern, and the linker generated is extremely stable. There were also no concerns of the instability of the alkyne-cGAMP compound. We were able to verify formation of the cGAMP-KLH (and BSA) conjugate, although indirectly, through two completely different methods. Even after freezing and thawing samples, the conjugate was still readily observed via these methods.

Even with a successfully conjugated compound in hand, one cannot guarantee a successful immunization. Technical error aside, the hapten component of the conjugate must be 'visible' to the immune system in order for any antibody production to occur. The azide we used

to modify the KLH compound, NHS-Peg4-Azide, links the azide group to the NHS group via a chain of four ethylene oxide groups, which ultimately generates more space between the cGAMP and KLH. Our hope in using this compound was that this improved the 'visibility' of cGAMP to the animal's immune system.

Our mouse immunizations with the click chemistry-generated complex seemed promising – the polyclonal sera were capable of recognizing 2'3'-cGAMP, and did so in a specific fashion (it did not bind measurably ATP, GTP, cdA, or cdG). Ultimately these antibodies bound biotinylated cGAMP, but confusingly, this binding could not be overcome by high concentrations of free 2'3'-cGAMP. Perhaps the antibodies recognized a specific epitope or conformation of the KLH-conjugated form of cGAMP, which differed from free 2'3'-cGAMP, or which was more like that of the biotinylated cGAMP coating the ELISA plate. It should also be noted that substantial time and effort was put into screening and subcloning hybridomas, and from over 2000 screened clones, less than 50 showed any response, and less than 10 were totally specific to 2'3'-cGAMP using the biotinylated-cGAMP ELISA. Perhaps it would have been beneficial to screen a larger number of clones, to obtain more positive hybridomas. It is possible that during culture some clones which were initially positive underwent genetic changes and lost the response – hybridomas are well-known for being finicky and sensitive. As mentioned in the introduction, rabbits often generate antibody responses to compounds which are non-immunogenic in mice; often, when a peptide or small molecule is used for immunization, rabbits are the preferred choice. With this in mind, we decided to move to a rabbit immunization strategy, which thankfully proved successful.

Sensitivity and specificity of the 2'3'-cGAMP antibody

Our antibody demonstrates a binding affinity to 2'3'-cGAMP in the low nanomolar range, a value generally accepted as high affinity for antibody-antigen binding. Studies into the specificity of antigen recognition found the antibody to be highly specific for 2'3'-cGAMP. In competition ELISA experiments, the antibody did show binding to 3'2'-cGAMP at relatively high concentrations of free competing compound, but almost no binding to the 2'2'-cGAMP isomer and none to the 3'3'-cGAMP isomer. It should be noted that 3'2'-cGAMP and 2'2'-cGAMP are not known to exist in nature, and 3'3'-cGAMP has only been identified in bacteria. We are now in the process of antibody affinity maturation, which will hopefully afford us with an antibody of higher sensitivity and possibly specificity.

The remarkable specificity of the antibody for 2'3'-cGAMP is sustainable even within the complex environment of the cell, which is valuable for future clinical applications. Because we ultimately hope to use this for detection of 2'3'-cGAMP within patient or animal samples, it is most important that the antibody be specific for 2'3'-cGAMP relative to other similar small molecules present in those samples. For mammals, and metazoans in general, such small molecules primarily include nucleotides and nucleosides, such as ATP, GTP, ADP, and GDP, and cyclic versions of these, such as cyclic AMP and cyclic GMP. The only scenario in which other cGAMP isomers may exist in mammalian samples is if the host happened to have an infection by a pathogen that is actively secreting CDNs into host cells; even in such a rare case, our antibody should be specific enough to pinpoint the endogenously produced 2'3'-cGAMP isomer.

In this study, we demonstrate the ability of this antibody to visualize 2'3'-cGAMP within cells, and serve as a valuable tool for further study of the pathway from a cell biology standpoint.

This is crucial because current methods to monitor 2'3'-cGAMP can only quantify the level produced in cells, but not assess its localization. Currently, we do not know how cGAMP is degraded within cells, if it localizes to certain compartments, or if/how it is exported from cells. Use of this antibody in future live-cell imaging experiments will aid in answering these and other key questions in the field concerning 2'3'-cGAMP signaling dynamics and clearance.

There is also a potential use for this antibody to study cGAMP localization in tissues, through immunohistochemistry. Previous studies of mice deficient in the exonuclease, TREX1, found 2'3'-cGAMP levels to be elevated in whole heart extract (using Mass Spectrometry techniques), and multiple tissues showed distinct inflammatory pathology and increased ISG expression – effects eliminated upon whole-body cGAS deletion. However, the exact cell population responsible for 2'3'-cGAMP production was not identified. Although we know the cGAS-STING pathway is present in both immune and non-immune cells, it is unknown whether the source of 2'3'-cGAMP from diseased mice hearts is the myocardium itself, or a small population of immune cells within the heart. A comprehensive immunohistochemical study of diseased tissue may thus uncover the cells contributing to the inflammatory phenotype in these mice. Such a technique can also be adapted to human pathology samples from multiple autoimmune diseases. One particular avenue of interest is that of dermatologic autoimmune conditions, such as Systemic Scleroderma and Psoriasis: patient samples can be easily obtained and studied, and protocols are well established for their immunohistochemical analysis. Along these lines, our successful use of the 2'3'-cGAMP antibody in flow cytometry and ImageStream methods will prove useful for future studies to distinguish between unique cell types producing 2'3'-cGAMP in a given heterogeneous mouse or patient sample.

As continuing evidence links numerous autoimmune and inflammatory diseases to alterations in the cGAS-STING pathway, it is imperative to develop a rapid and reliable assay for detecting the subset of patients who may benefit from the pathway's pharmacologic modulation. As referenced above, two studies have shown that 2'3'-cGAMP production is elevated in mice lacking Trex1, or DNaseII (Gao et al., 2015; Gray et al., 2015). Specifically, the study preformed in our lab quantified 2'3'-cGAMP production in hearts of three Trex1$^{-/-}$ mice, or Trex1$^{-/-}$STING$^{-/-}$ mice using Mass Spectrometry. Approximately 20 to 100 femtomoles was found in the Trex1$^{-/-}$ mice, and between 100 and 1000 femtomoles in the double knockout mice. In my hands, using the previously mentioned ELISA assays, I could not detect any elevated 2'3'-cGAMP production in the hearts of these mice. This could be due to technical or processing errors, but most likely the level of molecule produced is below the limit of detection for the antibody as it is used in a standard ELISA. Additionally, our lab has attempted to measure 2'3'-cGAMP levels in autoimmune mouse and human PBMCs using Mass Spectrometry, but we have not been able to detect a strong signal. This is in contrast to a study referenced earlier, in which a subset of lupus patients were shown to have elevated 2'3'-cGAMP levels (An et al., 2017). However, this study was not extensive and the 2'3'-cGAMP amount was not directly quantified. Further work is needed to improve the sensitivity of detection with our antibody such that it can be used for diagnosis of samples from autoimmune disease patients.

CHAPTER FOUR
METHODOLOGY

Antibodies

The following antibodies were used in this study: phospho-TBK1 and phospho-IRF3 (Cell Signaling), Flag (M2, Sigma-Aldrich), Tubulin (Sigma-Aldrich), HRP-linked anti-Rabbit IgG and HRP-linked anti-Mouse IgG (Cell Signaling), goat anti-rabbit IgG conjugated with Alexa Fluor 568 and goat anti-mouse IgG conjugated with Alexa Fluor 488 (Life Technologies).

Viral infection, cell culture, transfection

HSV (Δ34.5) virus was propagated in Vero cells and the resulting supernatant containing virus was used for infection, by direct addition to plated or suspension cells. An MOI of 5 or 10 was used for all experiments, as specified in figure legends. VSV (ΔM51) was propagated and used in the same fashion as HSV.

Cell lines were cultured at 37°C in an atmosphere of 5% (v/v) CO_2. All BJ, Hela, and MEF cell lines were cultured in Dulbecco's Modified Eagle's Medium (DMEM) supplemented with 10% (v/v) fetal bovine serum (Atlanta) and antibiotics. THP1 cells were cultured in RPMI 1640 supplemented with 10% fetal bovine serum, 2 mM β-mercaptoethanol, and antibiotics. Embryonic fibroblasts from WT or cGAS KO Mice were isolated from day 15.5 embryos and cultured in DMEM supplemented with 10% (vol/vol) FBS.

Plasmids and HT-DNA (Herring Testes DNA – Sigma Aldrich) were transfected into cells using Lipofectamine 2000 (Life Technologies).

Human and mouse PBMC isolation

Mouse blood was collected in tubes containing heparin. Human blood was obtained from healthy donors (Carter BloodCare Center, Dallas, Texas) in apheresis cones. Blood was diluted with PBS and cells were isolated using HISTOPAQUE 1083 (Sigma), according to the

manufacturer's instructions. Mouse samples were lysed using Red Blood Cell Lysis Buffer Hybri-max (Sigma) according to manufacturer's instructions. Isolated PMBCs were counted with a manual hemocytometer and used immediately in downstream experiments.

RNA Isolation and qRT-PCR

Total RNA was isolated and purified from cells using TRIzol according to manufacturer's guidelines (Invitrogen). Reverse transcription was performed using an iScript cDNA Synthesis Kit (Bio-Rad). qPCR samples were prepared with SYBR Green Supermix PCR kit (Bio-Rad), and qPCR was performed on an Applied Biosystems Viia7 Machine. The following primers were used: Human GAPDH Forward (*ATGACATCAAGAAGGTGGTG*), Human GAPDH Reverse (*CATACCAGGAAATGAGCTTG*), Human IFNβ Forward (*AGGACAGGATGAACTTTGAC*), Human IFNβ Reverse (*TGATAGACATTAGCCAGGAG*).

Heat Sup Preparation

As outlined previously (Gao et al., 2015), treated cells (nucleic acid transfected, virus infected, etc) were spun down at 3000 rpm for 3 minutes and washed once with PBS. The cells were then incubated for 5 minutes on ice in hypotonic buffer [10mM Tris HCl, 10nM KCl, 1mM MgCl2 (pH 7.3)], and lysed by passage 5 times through a 27.5G needle. The samples were spun at 14,000xg at 4°C for 10 minutes, and the supernatant was collected and boiled for 10 minutes at 98°C. This was spun down at 14,000xg for 10 minutes and the resulting supernatant was collected and stored at -80°C until needed.

2'3'-cGAMP extraction and Mass Spectrometry quantification

As outlined previously (Collins et al., 2015; Gao et al., 2015), 2'3'-cGAMP in heat sup was quantified using Mass Spectrometry. Briefly, 2'3'-cGAMP was enriched from the heat sup by solid-phase extraction (SPE) using HyperSep Aminopropyl SPE Columns (Thermo

Scientific). SPE eluents were separated with an Xbridge Amide column (3.5 µm, 3.5 mm ID × 100 mm L; Waters) on a Dionex Ultimate 3000 Rapid Separation Liquid Chromatography system (Thermo Scientific). Mobile phase A was 20 mM ammonium bicarbonate with 20 mM ammonium hydroxide in water, and mobile phase B was acetonitrile. The flow rate for separation was 400 µL/min for the first 14.5 min and 800 µL/min for the final 8.5 min, through the gradient: 0 min, 85% B; 3 min, 85% B; 10 min, 2% B; 14 min, 2% B; 14.5 min, 85% B; and 23 min, 85% B.

The LC eluent was ionized with an Ion Max NG heated electrospray source, using a spray voltage of +3,750 V; an ion transfer tube temperature of 342°C; a vaporizing temperature of 292 °C; and the sheath, auxiliary, and sweep gas at 45, 17, and 1 arbitrary units, respectively. The spray was analyzed online using a TSQ Quantiva triple quadruple mass spectrometer (Thermo Scientific), which performed continuous multiple reaction monitoring scans to detect 2'3'-cGAMP, as well as the internal standard. The technical details of the data acquisition and analysis were also described in the previously referenced work.

Fluorescence Microscopy

Immunostaining of cells for 2'3'-cGAMP was performed using a Tyramide SuperBoost Kit according to the manufacturer's instructions with slight modifications as described below (Invitrogen). Briefly, cells were first washed multiple times with PBS and then fixed using 4% Paraformaldehyde. Cells were then permeabilized using .1% Triton X-100 in PBS (PBS-T) for 15 minutes at room temperature. Endogenous peroxidase activity was quenched by incubating cells with 3% Hydrogen Peroxide solution for 1 hour at room temperature, followed by a blocking step with 5% BSA in PBS (with Triton X-100). Cells were first stained for STING by incubating with an antibody against Flag followed by goat anti-mouse IgG conjugated with

Alexa Fluor 488. After washing with PBS-T, cells were incubated with homemade rabbit antibody against 2'3'-cGAMP for 1 hour at room temperature, followed by incubation with anti-Rabbit IgG, HRP-linked antibody for 1 hour at room temperature. Cells were washed with PBS and then incubated for 10 minutes at room temperature with Alexa Fluor 568-labeled Tyramide reagent. Cells were then washed with PBS multiple times, and nuclei were stained with a DAPI-containing mounting medium (Vector Labs). Images were taken using a Zeiss LSM700 confocal microscope, and processed using a Zeiss LSM image browser.

FACS/ImageStream

Cells to be sorted were rinsed with PBS and then fixed using 4% Paraformaldehyde in a 1.5 mL Eppendorf tube. Cells were then permeabilized using .1% Saponin in PBS for 15 minutes at room temperature. After a blocking step with 5% BSA in .1% Saponin-PBS, cells were incubated with the homemade rabbit 2'3'-cGAMP antibody in blocking buffer overnight at 4°C, followed by incubation with secondary antibody: anti-rabbit IgG conjugated with Alexa Fluor 568 or 488. Cells were resuspended in 200 μL of PBS for downstream FACS experiments. Stained cells were analyzed with a FACS Calibur instrument (BD) and the FACS data analyzed using Flowjo software. Gating strategies are specified in figures or figure legends.

For ImageStream experiments, the above protocol was used with the following addition: after treatment with secondary antibody, cells were incubated at room temperature for 10 minutes with 20uM DRAQ5 (Thermo Scientific) in PBS, and finally resuspended in 20 μL of PBS for downstream Imagestream experiments. Images of stained cells were acquired using an ImageStreamMarkII Flow Cytometer (Amnis), and acquired images were analyzed with Amnis software (IDEAS).

Antigen Preparation

Two carrier protein – cGAMP conjugates were generated for immunization: mcKLH-conjugated cGAMP (KLH-cGAMP) and BSA-conjugated cGAMP (BSA-cGAMP).

Carrier protein derivatization. Carrier proteins were first covalently modified by addition of azide functional groups to available primary amine residues (lysine residues). Briefly, the carrier protein (Imject Mariculture KLH or Imject Bovine Sera Albumin, Thermo Scientific) was incubated with a molar excess of NHS-PEG4-Azide (Thermo Scientific) in PBS (Dulbecco's Phosphate Buffered Saline, Sigma-Aldrich) for 30 minutes at room temperature, and then quenched with Tris-HCl (pH 8) for 5 minutes at room temperature. The resulting product was then purified on a 7K MWCO Zeba Spin Desalting Column (Thermo Scientific) pre-equilibrated with PBS, and stored at -80°C until needed.

Carrier – hapten conjugation using Click Chemistry. The derivatized carrier protein ("azide-KLH" or "azide-BSA") was covalently conjugated to the hapten, alkyne-cGAMP, using standard click chemistry techniques. Briefly, KLH-azide and cGAMP-alkyne were combined in PBS, with cGAMP-alkyne in molar excess. A catalyst mixture was prepared [1.7 mM Tris(benzyltriazolylmethyl) amine (TBTA) in 80% *tert*-Butanol/20% DMSO, 50 mM $CuSO_4$ in H_2O, and 50 mM tris-carboxyethyl phosphine (TCEP) in H_2O (pH 7)] and immediately added to the reaction. The reaction was incubated for 15 minutes at room temperature, purified on a PBS-equilibrated Zeba Spin Desalting Column, and stored at -80°C until needed. All components of the catalyst mix were purchased individually from Sigma-Adrich.

Mouse Immunization and blood collection

Timeline. Four female BALB/c mice (Jackson Labs) were immunized over the course of 45 days, and bled periodically throughout to test for a positive antibody response. An initial

bleed was performed before immunization as a control, followed by bleeds at day 21 and 35 after the initial bleed. A terminal bleed was performed on day 45 (along with spleen harvest). The total volume of blood collected each time approximated 100 µLs, collected from the facial vein (punctured using a lancet). For immunization, mice were subject to an initial intramuscular injection of 100 µg of KLH-cGAMP emulsified with Freund's Complete Adjuvant (FCA, Sigma), followed by 2 boost injections intramuscularly of 50 µg KLH-cGAMP emulsified with Freund's Incomplete Adjuvant (ICA, Sigma) at days 14 and 28. A final boost was given intravenously with 50 µg KLH-cGAMP in ICA on day 42 (three days prior to spleen harvest).

Antigen preparation and injection. To generate antigen for injection, the carrier protein-cGAMP conjugate (in PBS) was emulsified by manually mixing with an equal volume of Freund's Adjuvant (FCA or ICA) for 20 minutes in a hand-held emulsifier.

Rabbit Immunization and blood collection

Timeline. Two New Zealand White Rabbits (Charles River) were immunized over the course of 11 weeks, and bled periodically throughout to test for a positive antibody response. An initial bleed was performed before immunization as a control, followed by bleeds 3, 7, 8, and 11 weeks after the initial bleed. The total volume of blood collected each time approximated 5 mLs. For immunization, rabbits were subject to an initial injection of .5 mg of KLH-cGAMP emulsified with Freund's Complete Adjuvant (FCA, Sigma), followed by 2 boost injections of .25 mg KLH-cGAMP emulsified with Freund's Incomplete Adjuvant (ICA, Sigma) at 2 and 4 weeks after the first injection, and an additional 3 boost injections with .25 mg BSA-cGAMP emulsified with ICA at 6, 8, and 11 weeks after the first injection.

Antigen preparation and injection. To generate antigen for injection into rabbits, the carrier protein-cGAMP conjugate (in PBS) was emulsified by manually mixing with an equal

volume of Freund's Adjuvant (FCA or ICA) for 20 minutes in a hand-held emulsifier. The resulting emulsion was injected subcutaneously at up to three sites on the rabbit's back, with up to .2 mL per injection site. The first immunization totaled approximately .6 mL emulsion per rabbit, and the subsequent boost injections were between .2 and .4 mL emulsion per rabbit.

Verification of polyclonal antibody response

Rabbit and Mouse Sera Collection. Rabbit or mouse whole blood was collected, allowed to clot, and then spun down at 4000 rpm for 25 minutes. The top clear layer (sera) was collected and stored at -80°C until needed.

ELISA to verify antibody response. A Pierce Streptavidin Coated ELISA plate (Thermo Scientific) was washed 3 times with wash buffer [.1% BSA (Sigma) in TBS-T (Tris Buffered Saline containing .05% Tween-20)] and coated with .5 pmols/well of a biotinylated analog of cGAMP (c[8-Biotin-11-G(2',5')pA(3',5')p], Biolog) for 3 hours at room temperature. After washing the plate 3 times with wash buffer, varying dilutions of sera in the wash buffer were added to each well and allowed to incubate overnight at 4°C. The plate was again washed 3 times and secondary antibody (Anti-Rabbit IgG or Anti-Mouse IgG, HRP-linked Antibody, Cell Signaling Technology) diluted in wash buffer was added for 1 hour at room temperature. The plate was washed at least three times with wash buffer, and developed using TMB Substrate Solution according to the manufacturer's instructions (Thermo Scientific). The reaction was quenched with .16M H_2SO_4 after an appropriate amount of color change was noted. $OD450_{nm}$ values were obtained using a Multiskan MCC/340 Plate Reader (ThermoFisher Scientific).

As a control to verify response to the carrier protein, ELISA plates were conjugated using either KLH or BSA, as follows: A common flat bottom 96-well ELISA plate was rehydrated with coating buffer [0.2 M sodium carbonate/bicarbonate buffer, pH 9.6] and coated with 50

ul/well of a 20 ug/mL solution of carrier protein for 2 hours at room temperature. The plate was washed three times with wash buffer [.1% BSA (Sigma) in PBS-T (PBS containing .05% Tween-20)] and blocked with 5% BSA in PBS-T for 1 hour at room temperature. After washing the plate 3 times with wash buffer, varying dilutions of sera in the wash buffer were added to each well and allowed to incubate overnight at 4°C. The plate was again washed 3 times and secondary antibody (Anti-rabbit IgG or Anti-mouse IgG, HRP-linked Antibody, Cell Signaling Technology) diluted in wash buffer was added for 1 hour at room temperature. The plate was washed again at least three times with wash buffer, and developed using TMB Substrate Solution (Thermo Scientific). The reaction was quenched with .16M H_2SO_4 after an appropriate amount of color change was noted. $OD450_{nm}$ values were obtained using a Multiskan MCC/340 Plate Reader (ThermoFisher Scientific).

Competitive ELISA/functional assay. To determine the approximate IC50 values of 2'3'-cGAMP binding to rabbit polyclonal sera and isolated single clones, as well as the IC_{50} values for other cGAMP analogs (2'2'-cGAMP, 3'3'-cGAMP, 3'2'-cGAMP), cyclic dinucleotides (Cyclic-di-AMP, Cyclic-di-GMP) and relevant small molecules (ATP/ADP/GTP/GDP), a competitive ELISA assay was performed. As previously mentioned, a Pierce Streptavidin Coated ELISA plate was washed 3 times with wash buffer [.1% BSA (Sigma) in TBS-T (Tris Buffered Saline containing .05% Tween-20)] and coated with .5 pmols/well of biotinylated cGAMP for 3 hours at room temperature. Meanwhile, either polyclonal sera, isolated supernatant containing antibodies from a single clone, or purified antibody from a single clone (diluted to 50 uL in wash buffer) was incubated with varying concentrations of small molecule (diluted to 50 uL in wash buffer) for 1 hour at room temperature. The mixtures were added to individual wells and allowed to incubate overnight at 4°C. The plate was again washed 3 times and secondary

antibody (Anti-Rabbit IgG or Anti-Mouse IgG, HRP-linked Antibody, Cell Signaling Technology) diluted in wash buffer was added for 1 hour at room temperature. The plate was washed at least three times with wash buffer, and developed using TMB Substrate Solution (Thermo Scientific) according to manufacturer guidelines. The reaction was quenched with .16M H_2SO_4 after an appropriate amount of color change was noted. $OD450_{nm}$ values were obtained using a Multiskan MCC/340 Plate Reader (ThermoFisher Scientific). Graphpad's Prism 7 software was used to generate and fit IC_{50} curves for each small molecule.

2'3'-cGAMP was purchased from Pharmaron. 3'3'-cGAMP, 3'2-cGAMP, 2'2'-cGAMP, Cyclic-di-AMP and Cyclic-di-GMP were all purchased from Biolog. ATP, ADP, GTP, GDP were purchased from Sigma Aldrich. Biotinylated cGAMP (c[8-Biotin-11-G(2',5')pA(3',5')p]) was purchased from Biolog.

Rabbit PBMC isolation

Approximately 10 mL of blood was collected from the immunized rabbit into a blood collection tube containing heparin. The blood was diluted 1:1 with room temperature PBS and then carefully added to a 50 mL conical tube containing 15 mL of room temperature lymphocyte separation media (LSM, Corning) so as not to disturb the interface between layers. The tube was then centrifuged at 1500 rpm at room temperature for 30 minutes, and the resulting layer of PBMCs was transferred into a new 50 mL conical tube. The PBMCs were rinsed with PBS and centrifuged for 10 minutes at 1100 rpm, twice. The cells were then re-suspended in 5 mLs of RPMI media supplemented with 10% Fetal Bovine Serum and antibiotic/antimycotic, and 45 additional mL of media was added to fill the tube.

Rabbit monoclonal antibody isolation

As outlined in Chapter Two, the isolation of monoclonal rabbit antibodies against 2'3'-cGAMP required a considerable amount of screening steps. Isolated PBMCs from immunized rabbits were shipped to a collaborating company, RevMab Biosciences, USA. The company offers technology that does not require hybridoma generation, and instead use proprietary methods to extend the lifespan of antibody-producing B-cells long enough to collect a testable amount of antibody. Although the B-cells cannot be saved or grown indefinitely, RNA can easily be isolated from the cells, and the genetic material can be sequenced for downstream cloning. RevMab Biosciences performed the initial ELISA screening of over 700 B-cell supernatants, and found 123 clones to be positive. We further tested these clones and chose 20 with the best activity in competition ELISA assay. Our collaborator, Dr. Mark Gui from Dr. Zhiqiang An's lab at the University of Texas at Houston, performed the cloning of all 20 antibodies with robust performance in the competition assay.

Mouse monoclonal antibody generation

To generate mouse monoclonal antibodies, a ClonaCell-HY Hybridoma Cloning Kit was used (STEMCELL Technologies). Spleen harvest and B-cell isolation, along with hybridoma formation, hybridoma selection, hybridoma supernatant screening, and hybridoma subcloning were followed exactly as indicated in the kit's manual. The myeloma cell line used was P3X63Ag8.653 (ATCC CRL-1580), and was cultured according to the company's guidelines.

CHAPTER FIVE
BIBLIOGRAPHY

Ablasser, A., Goldeck, M., Cavlar, T., Deimling, T., Witte, G., Rohl, I., . . . Hornung, V. (2013). cGAS produces a 2'-5'-linked cyclic dinucleotide second messenger that activates STING. *Nature, 498*(7454), 380-384. doi:10.1038/nature12306

Ablasser, A., Schmid-Burgk, J. L., Hemmerling, I., Horvath, G. L., Schmidt, T., Latz, E., & Hornung, V. (2013). Cell intrinsic immunity spreads to bystander cells via the intercellular transfer of cGAMP. *Nature, 503*(7477), 530-534. doi:10.1038/nature12640

Aguirre, S., Luthra, P., Sanchez-Aparicio, M. T., Maestre, A. M., Patel, J., Lamothe, F., . . . Fernandez-Sesma, A. (2017). Dengue virus NS2B protein targets cGAS for degradation and prevents mitochondrial DNA sensing during infection. *Nat Microbiol, 2*, 17037. doi:10.1038/nmicrobiol.2017.37

Ahmad-Nejad, P., Hacker, H., Rutz, M., Bauer, S., Vabulas, R. M., & Wagner, H. (2002). Bacterial CpG-DNA and lipopolysaccharides activate Toll-like receptors at distinct cellular compartments. *Eur J Immunol, 32*(7), 1958-1968. doi:10.1002/1521-4141(200207)32:7<1958::AID-IMMU1958>3.0.CO;2-U

Ahmed, R., & Gray, D. (1996). Immunological memory and protective immunity: understanding their relation. *Science, 272*(5258), 54-60.

Aicardi, J., & Goutieres, F. (1984). A progressive familial encephalopathy in infancy with calcifications of the basal ganglia and chronic cerebrospinal fluid lymphocytosis. *Ann Neurol, 15*(1), 49-54. doi:10.1002/ana.410150109

Alexopoulou, L., Holt, A. C., Medzhitov, R., & Flavell, R. A. (2001). Recognition of double-stranded RNA and activation of NF-kappaB by Toll-like receptor 3. *Nature, 413*(6857), 732-738. doi:10.1038/35099560

An, J., Durcan, L., Karr, R. M., Briggs, T. A., Rice, G. I., Teal, T. H., . . . Elkon, K. B. (2017). Expression of Cyclic GMP-AMP Synthase in Patients With Systemic Lupus Erythematosus. *Arthritis Rheumatol, 69*(4), 800-807. doi:10.1002/art.40002

Andrade, W. A., Agarwal, S., Mo, S., Shaffer, S. A., Dillard, J. P., Schmidt, T., . . . Golenbock, D. T. (2016). Type I Interferon Induction by Neisseria gonorrhoeae: Dual Requirement of Cyclic GMP-AMP Synthase and Toll-like Receptor 4. *Cell Rep, 15*(11), 2438-2448. doi:10.1016/j.celrep.2016.05.030

Andrade, W. A., Firon, A., Schmidt, T., Hornung, V., Fitzgerald, K. A., Kurt-Jones, E. A., . . . Kaminski, P. A. (2016). Group B Streptococcus Degrades Cyclic-di-AMP to Modulate STING-Dependent Type I Interferon Production. *Cell Host Microbe, 20*(1), 49-59. doi:10.1016/j.chom.2016.06.003

Bonilla, F. A., & Oettgen, H. C. (2010). Adaptive immunity. *J Allergy Clin Immunol, 125*(2 Suppl 2), S33-40. doi:10.1016/j.jaci.2009.09.017

Bose, D., Su, Y., Marcus, A., Raulet, D. H., & Hammond, M. C. (2016). An RNA-Based Fluorescent Biosensor for High-Throughput Analysis of the cGAS-cGAMP-STING Pathway. *Cell Chem Biol, 23*(12), 1539-1549. doi:10.1016/j.chembiol.2016.10.014

Bridgeman, A., Maelfait, J., Davenne, T., Partridge, T., Peng, Y., Mayer, A., . . . Rehwinkel, J. (2015). Viruses transfer the antiviral second messenger cGAMP between cells. *Science, 349*(6253), 1228-1232. doi:10.1126/science.aab3632

Burdette, D. L., Monroe, K. M., Sotelo-Troha, K., Iwig, J. S., Eckert, B., Hyodo, M., . . . Vance, R. E. (2011). STING is a direct innate immune sensor of cyclic di-GMP. *Nature, 478*(7370), 515-518. doi:10.1038/nature10429

Burhenne, H., & Kaever, V. (2013). Quantification of cyclic dinucleotides by reversed-phase LC-MS/MS. *Methods Mol Biol, 1016*, 27-37. doi:10.1007/978-1-62703-441-8_3

Civril, F., Deimling, T., de Oliveira Mann, C. C., Ablasser, A., Moldt, M., Witte, G., . . . Hopfner, K. P. (2013). Structural mechanism of cytosolic DNA sensing by cGAS. *Nature, 498*(7454), 332-337. doi:10.1038/nature12305

Collins, A. C., Cai, H., Li, T., Franco, L. H., Li, X. D., Nair, V. R., . . . Shiloh, M. U. (2015). Cyclic GMP-AMP Synthase Is an Innate Immune DNA Sensor for Mycobacterium tuberculosis. *Cell Host Microbe, 17*(6), 820-828. doi:10.1016/j.chom.2015.05.005

Corrigan, R. M., & Grundling, A. (2013). Cyclic di-AMP: another second messenger enters the fray. *Nat Rev Microbiol, 11*(8), 513-524. doi:10.1038/nrmicro3069

Crow, Y. J. (2011). Type I interferonopathies: a novel set of inborn errors of immunity. *Ann N Y Acad Sci, 1238*, 91-98. doi:10.1111/j.1749-6632.2011.06220.x

Crow, Y. J., Chase, D. S., Lowenstein Schmidt, J., Szynkiewicz, M., Forte, G. M., Gornall, H. L., . . . Rice, G. I. (2015). Characterization of human disease phenotypes associated with mutations in TREX1, RNASEH2A, RNASEH2B, RNASEH2C, SAMHD1, ADAR, and IFIH1. *Am J Med Genet A, 167A*(2), 296-312. doi:10.1002/ajmg.a.36887

Crowl, J. T., Gray, E. E., Pestal, K., Volkman, H. E., & Stetson, D. B. (2017). Intracellular Nucleic Acid Detection in Autoimmunity. *Annu Rev Immunol, 35*, 313-336. doi:10.1146/annurev-immunol-051116-052331

Davies, B. W., Bogard, R. W., Young, T. S., & Mekalanos, J. J. (2012). Coordinated regulation of accessory genetic elements produces cyclic di-nucleotides for V. cholerae virulence. *Cell, 149*(2), 358-370. doi:10.1016/j.cell.2012.01.053

Dey, R. J., Dey, B., Zheng, Y., Cheung, L. S., Zhou, J., Sayre, D., . . . Bishai, W. R. (2017). Inhibition of innate immune cytosolic surveillance by an M. tuberculosis phosphodiesterase. *Nat Chem Biol, 13*(2), 210-217. doi:10.1038/nchembio.2254

Diebold, S. S., Kaisho, T., Hemmi, H., Akira, S., & Reis e Sousa, C. (2004). Innate antiviral responses by means of TLR7-mediated recognition of single-stranded RNA. *Science, 303*(5663), 1529-1531. doi:10.1126/science.1093616

Diner, E. J., Burdette, D. L., Wilson, S. C., Monroe, K. M., Kellenberger, C. A., Hyodo, M., . . . Vance, R. E. (2013). The innate immune DNA sensor cGAS produces a noncanonical cyclic dinucleotide that activates human STING. *Cell Rep, 3*(5), 1355-1361. doi:10.1016/j.celrep.2013.05.009

Ding, L., Dong, G., Zhang, D., Ni, Y., & Hou, Y. (2015). The regional function of cGAS/STING signal in multiple organs: One of culprit behind systemic lupus erythematosus? *Med Hypotheses, 85*(6), 846-849. doi:10.1016/j.mehy.2015.09.026

Dobbs, N., Burnaevskiy, N., Chen, D., Gonugunta, V. K., Alto, N. M., & Yan, N. (2015). STING Activation by Translocation from the ER Is Associated with Infection and Autoinflammatory Disease. *Cell Host Microbe, 18*(2), 157-168. doi:10.1016/j.chom.2015.07.001

Ettinger, R., Sims, G. P., Fairhurst, A. M., Robbins, R., da Silva, Y. S., Spolski, R., . . . Lipsky, P. E. (2005). IL-21 induces differentiation of human naive and memory B cells into antibody-secreting plasma cells. *J Immunol, 175*(12), 7867-7879.

Feng, L., Wang, X., & Jin, H. (2011). Rabbit monoclonal antibody: potential application in cancer therapy. *Am J Transl Res, 3*(3), 269-274.

Gao, D., Li, T., Li, X. D., Chen, X., Li, Q. Z., Wight-Carter, M., & Chen, Z. J. (2015). Activation of cyclic GMP-AMP synthase by self-DNA causes autoimmune diseases. *Proc Natl Acad Sci U S A, 112*(42), E5699-5705. doi:10.1073/pnas.1516465112

Gao, D., Wu, J., Wu, Y. T., Du, F., Aroh, C., Yan, N., . . . Chen, Z. J. (2013). Cyclic GMP-AMP synthase is an innate immune sensor of HIV and other retroviruses. *Science, 341*(6148), 903-906. doi:10.1126/science.1240933

Gao, P., Ascano, M., Wu, Y., Barchet, W., Gaffney, B. L., Zillinger, T., . . . Patel, D. J. (2013). Cyclic [G(2',5')pA(3',5')p] is the metazoan second messenger produced by DNA-activated cyclic GMP-AMP synthase. *Cell, 153*(5), 1094-1107. doi:10.1016/j.cell.2013.04.046

Gentili, M., Kowal, J., Tkach, M., Satoh, T., Lahaye, X., Conrad, C., . . . Manel, N. (2015). Transmission of innate immune signaling by packaging of cGAMP in viral particles. *Science, 349*(6253), 1232-1236. doi:10.1126/science.aab3628

Gray, E. E., Treuting, P. M., Woodward, J. J., & Stetson, D. B. (2015). Cutting Edge: cGAS Is Required for Lethal Autoimmune Disease in the Trex1-Deficient Mouse Model of Aicardi-Goutieres Syndrome. *J Immunol, 195*(5), 1939-1943. doi:10.4049/jimmunol.1500969

Gurtler, C., & Bowie, A. G. (2013). Innate immune detection of microbial nucleic acids. *Trends Microbiol, 21*(8), 413-420. doi:10.1016/j.tim.2013.04.004

Hacker, H., Vabulas, R. M., Takeuchi, O., Hoshino, K., Akira, S., & Wagner, H. (2000). Immune cell activation by bacterial CpG-DNA through myeloid differentiation marker 88 and tumor necrosis factor receptor-associated factor (TRAF)6. *J Exp Med, 192*(4), 595-600.

Hallberg, Z. F., Wang, X. C., Wright, T. A., Nan, B., Ad, O., Yeo, J., & Hammond, M. C. (2016). Hybrid promiscuous (Hypr) GGDEF enzymes produce cyclic AMP-GMP (3', 3'-cGAMP). *Proc Natl Acad Sci U S A, 113*(7), 1790-1795. doi:10.1073/pnas.1515287113

Hansen, K., Prabakaran, T., Laustsen, A., Jorgensen, S. E., Rahbaek, S. H., Jensen, S. B., . . . Paludan, S. R. (2014). Listeria monocytogenes induces IFNbeta expression through an IFI16-, cGAS- and STING-dependent pathway. *EMBO J, 33*(15), 1654-1666. doi:10.15252/embj.201488029

Hayashi, F., Smith, K. D., Ozinsky, A., Hawn, T. R., Yi, E. C., Goodlett, D. R., . . . Aderem, A. (2001). The innate immune response to bacterial flagellin is mediated by Toll-like receptor 5. *Nature, 410*(6832), 1099-1103. doi:10.1038/35074106

He, J., Hao, R., Liu, D., Liu, X., Wu, S., Guo, S., . . . Guo, D. (2016). Inhibition of hepatitis B virus replication by activation of the cGAS-STING pathway. *J Gen Virol, 97*(12), 3368-3378. doi:10.1099/jgv.0.000647

Heil, F., Hemmi, H., Hochrein, H., Ampenberger, F., Kirschning, C., Akira, S., . . . Bauer, S. (2004). Species-specific recognition of single-stranded RNA via toll-like receptor 7 and 8. *Science, 303*(5663), 1526-1529. doi:10.1126/science.1093620

Hemmi, H., Takeuchi, O., Kawai, T., Kaisho, T., Sato, S., Sanjo, H., . . . Akira, S. (2000). A Toll-like receptor recognizes bacterial DNA. *Nature, 408*(6813), 740-745. doi:10.1038/35047123

Hermanson, G. T. (2013). *Bioconjugate Techniques*: Academic Press.

Hornung, V., Rothenfusser, S., Britsch, S., Krug, A., Jahrsdorfer, B., Giese, T., . . . Hartmann, G. (2002). Quantitative expression of toll-like receptor 1-10 mRNA in cellular subsets of human peripheral blood mononuclear cells and sensitivity to CpG oligodeoxynucleotides. *J Immunol, 168*(9), 4531-4537.

Huang, Y. H., Liu, X. Y., Du, X. X., Jiang, Z. F., & Su, X. D. (2012). The structural basis for the sensing and binding of cyclic di-GMP by STING. *Nat Struct Mol Biol, 19*(7), 728-730. doi:10.1038/nsmb.2333

Ishii, K. J., Coban, C., Kato, H., Takahashi, K., Torii, Y., Takeshita, F., . . . Akira, S. (2006). A Toll-like receptor-independent antiviral response induced by double-stranded B-form DNA. *Nat Immunol, 7*(1), 40-48. doi:10.1038/ni1282

Ishikawa, H., & Barber, G. N. (2008). STING is an endoplasmic reticulum adaptor that facilitates innate immune signalling. *Nature, 455*(7213), 674-678. doi:10.1038/nature07317

Ishikawa, H., Ma, Z., & Barber, G. N. (2009). STING regulates intracellular DNA-mediated, type I interferon-dependent innate immunity. *Nature, 461*(7265), 788-792. doi:10.1038/nature08476

Janeway, C. A., Jr., & Medzhitov, R. (2002). Innate immune recognition. *Annu Rev Immunol, 20*, 197-216. doi:10.1146/annurev.immunol.20.083001.084359

Jenal, U., Reinders, A., & Lori, C. (2017). Cyclic di-GMP: second messenger extraordinaire. *Nat Rev Microbiol, 15*(5), 271-284. doi:10.1038/nrmicro.2016.190

Jeremiah, N., Neven, B., Gentili, M., Callebaut, I., Maschalidi, S., Stolzenberg, M. C., . . . Rieux-Laucat, F. (2014). Inherited STING-activating mutation underlies a familial inflammatory syndrome with lupus-like manifestations. *J Clin Invest, 124*(12), 5516-5520. doi:10.1172/JCI79100

Jin, L., Waterman, P. M., Jonscher, K. R., Short, C. M., Reisdorph, N. A., & Cambier, J. C. (2008). MPYS, a novel membrane tetraspanner, is associated with major histocompatibility complex class II and mediates transduction of apoptotic signals. *Mol Cell Biol, 28*(16), 5014-5026. doi:10.1128/MCB.00640-08

Jin, M. S., Kim, S. E., Heo, J. Y., Lee, M. E., Kim, H. M., Paik, S. G., . . . Lee, J. O. (2007). Crystal structure of the TLR1-TLR2 heterodimer induced by binding of a tri-acylated lipopeptide. *Cell, 130*(6), 1071-1082. doi:10.1016/j.cell.2007.09.008

Kadowaki, N., Ho, S., Antonenko, S., Malefyt, R. W., Kastelein, R. A., Bazan, F., & Liu, Y. J. (2001). Subsets of human dendritic cell precursors express different toll-like receptors and respond to different microbial antigens. *J Exp Med, 194*(6), 863-869.

Kawai, T., & Akira, S. (2009). The roles of TLRs, RLRs and NLRs in pathogen recognition. *Int Immunol, 21*(4), 317-337. doi:10.1093/intimm/dxp017

Kellenberger, C. A., Wilson, S. C., Sales-Lee, J., & Hammond, M. C. (2013). RNA-based fluorescent biosensors for live cell imaging of second messengers cyclic di-GMP and cyclic AMP-GMP. *J Am Chem Soc, 135*(13), 4906-4909. doi:10.1021/ja311960g

Kohler, G., & Milstein, C. (1975). Continuous cultures of fused cells secreting antibody of predefined specificity. *Nature, 256*(5517), 495-497.

Kolb, H. C., Finn, M. G., & Sharpless, K. B. (2001). Click Chemistry: Diverse Chemical Function from a Few Good Reactions. *Angew Chem Int Ed Engl, 40*(11), 2004-2021.

Konig, N., Fiehn, C., Wolf, C., Schuster, M., Cura Costa, E., Tungler, V., . . . Lee-Kirsch, M. A. (2017). Familial chilblain lupus due to a gain-of-function mutation in STING. *Ann Rheum Dis, 76*(2), 468-472. doi:10.1136/annrheumdis-2016-209841

Kranzusch, P. J., Lee, A. S., Berger, J. M., & Doudna, J. A. (2013). Structure of human cGAS reveals a conserved family of second-messenger enzymes in innate immunity. *Cell Rep, 3*(5), 1362-1368. doi:10.1016/j.celrep.2013.05.008

Kranzusch, P. J., Wilson, S. C., Lee, A. S., Berger, J. M., Doudna, J. A., & Vance, R. E. (2015). Ancient Origin of cGAS-STING Reveals Mechanism of Universal 2',3' cGAMP Signaling. *Mol Cell, 59*(6), 891-903. doi:10.1016/j.molcel.2015.07.022

Krasteva, P. V., & Sondermann, H. (2017). Versatile modes of cellular regulation via cyclic dinucleotides. *Nat Chem Biol, 13*(4), 350-359. doi:10.1038/nchembio.2337

Landry, J. P., Ke, Y., Yu, G. L., & Zhu, X. D. (2015). Measuring affinity constants of 1450 monoclonal antibodies to peptide targets with a microarray-based label-free assay platform. *J Immunol Methods, 417*, 86-96. doi:10.1016/j.jim.2014.12.011

Leenaars, M., & Hendriksen, C. F. (2005). Critical steps in the production of polyclonal and monoclonal antibodies: evaluation and recommendations. *ILAR J, 46*(3), 269-279.

Li, L., Yin, Q., Kuss, P., Maliga, Z., Millan, J. L., Wu, H., & Mitchison, T. J. (2014). Hydrolysis of 2'3'-cGAMP by ENPP1 and design of nonhydrolyzable analogs. *Nat Chem Biol, 10*(12), 1043-1048. doi:10.1038/nchembio.1661

Li, X., Shu, C., Yi, G., Chaton, C. T., Shelton, C. L., Diao, J., . . . Li, P. (2013). Cyclic GMP-AMP synthase is activated by double-stranded DNA-induced oligomerization. *Immunity, 39*(6), 1019-1031. doi:10.1016/j.immuni.2013.10.019

Li, X. D., & Chen, Z. J. (2012). Sequence specific detection of bacterial 23S ribosomal RNA by TLR13. *Elife, 1*, e00102. doi:10.7554/eLife.00102

Li, X. D., Wu, J., Gao, D., Wang, H., Sun, L., & Chen, Z. J. (2013). Pivotal roles of cGAS-cGAMP signaling in antiviral defense and immune adjuvant effects. *Science, 341*(6152), 1390-1394. doi:10.1126/science.1244040

Liguori, M. J., Hoff-Velk, J. A., & Ostrow, D. H. (2001). Recombinant human interleukin-6 enhances the immunoglobulin secretion of a rabbit-rabbit hybridoma. *Hybridoma, 20*(3), 189-198. doi:10.1089/027245701750293529

Lio, C. W., McDonald, B., Takahashi, M., Dhanwani, R., Sharma, N., Huang, J., . . . Sharma, S. (2016). cGAS-STING Signaling Regulates Initial Innate Control of Cytomegalovirus Infection. *J Virol, 90*(17), 7789-7797. doi:10.1128/JVI.01040-16

Liu, Y., Jesus, A. A., Marrero, B., Yang, D., Ramsey, S. E., Montealegre Sanchez, G. A., . . . Goldbach-Mansky, R. (2014). Activated STING in a vascular and pulmonary syndrome. *N Engl J Med, 371*(6), 507-518. doi:10.1056/NEJMoa1312625

Livingston, J. H., & Crow, Y. J. (2016). Neurologic Phenotypes Associated with Mutations in TREX1, RNASEH2A, RNASEH2B, RNASEH2C, SAMHD1, ADAR1, and IFIH1: Aicardi-Goutieres Syndrome and Beyond. *Neuropediatrics, 47*(6), 355-360. doi:10.1055/s-0036-1592307

Llewelyn, M. B., Hawkins, R. E., & Russell, S. J. (1992). Discovery of antibodies. *BMJ, 305*(6864), 1269-1272.

Lolicato, M., Bucchi, A., Arrigoni, C., Zucca, S., Nardini, M., Schroeder, I., . . . Moroni, A. (2014). Cyclic dinucleotides bind the C-linker of HCN4 to control channel cAMP responsiveness. *Nat Chem Biol, 10*(6), 457-462. doi:10.1038/nchembio.1521

Lund, J. M., Alexopoulou, L., Sato, A., Karow, M., Adams, N. C., Gale, N. W., . . . Flavell, R. A. (2004). Recognition of single-stranded RNA viruses by Toll-like receptor 7. *Proc Natl Acad Sci U S A, 101*(15), 5598-5603. doi:10.1073/pnas.0400937101

Mackenzie, K. J., Carroll, P., Lettice, L., Tarnauskaite, Z., Reddy, K., Dix, F., . . . Jackson, A. P. (2016). Ribonuclease H2 mutations induce a cGAS/STING-dependent innate immune response. *EMBO J, 35*(8), 831-844. doi:10.15252/embj.201593339

Mackinnon, A. L., & Taunton, J. (2009). Target Identification by Diazirine Photo-Cross-linking and Click Chemistry. *Curr Protoc Chem Biol, 1*, 55-73. doi:10.1002/9780470559277.ch090167

Maelfait, J., Bridgeman, A., Benlahrech, A., Cursi, C., & Rehwinkel, J. (2016). Restriction by SAMHD1 Limits cGAS/STING-Dependent Innate and Adaptive Immune Responses to HIV-1. *Cell Rep, 16*(6), 1492-1501. doi:10.1016/j.celrep.2016.07.002

Morita, M., Stamp, G., Robins, P., Dulic, A., Rosewell, I., Hrivnak, G., . . . Barnes, D. E. (2004). Gene-targeted mice lacking the Trex1 (DNase III) 3'-->5' DNA exonuclease develop inflammatory myocarditis. *Mol Cell Biol, 24*(15), 6719-6727. doi:10.1128/MCB.24.15.6719-6727.2004

Nishiya, T., & DeFranco, A. L. (2004). Ligand-regulated chimeric receptor approach reveals distinctive subcellular localization and signaling properties of the Toll-like receptors. *J Biol Chem, 279*(18), 19008-19017. doi:10.1074/jbc.M311618200

O'Neill, L. A., Golenbock, D., & Bowie, A. G. (2013). The history of Toll-like receptors - redefining innate immunity. *Nat Rev Immunol, 13*(6), 453-460. doi:10.1038/nri3446

Ouyang, S., Song, X., Wang, Y., Ru, H., Shaw, N., Jiang, Y., . . . Liu, Z. J. (2012). Structural analysis of the STING adaptor protein reveals a hydrophobic dimer interface and mode of cyclic di-GMP binding. *Immunity, 36*(6), 1073-1086. doi:10.1016/j.immuni.2012.03.019

Paijo, J., Doring, M., Spanier, J., Grabski, E., Nooruzzaman, M., Schmidt, T., . . . Kalinke, U. (2016). cGAS Senses Human Cytomegalovirus and Induces Type I Interferon Responses in Human Monocyte-Derived Cells. *PLoS Pathog, 12*(4), e1005546. doi:10.1371/journal.ppat.1005546

Poltorak, A., He, X., Smirnova, I., Liu, M. Y., Van Huffel, C., Du, X., . . . Beutler, B. (1998). Defective LPS signaling in C3H/HeJ and C57BL/10ScCr mice: mutations in Tlr4 gene. *Science, 282*(5396), 2085-2088.

Rajewsky, K., Schirrmacher, V., Nase, S., & Jerne, N. K. (1969). The requirement of more than one antigenic determinant for immunogenicity. *J Exp Med, 129*(6), 1131-1143.

Ross, P., Weinhouse, H., Aloni, Y., Michaeli, D., Weinberger-Ohana, P., Mayer, R., . . . Benziman, M. (1987). Regulation of cellulose synthesis in Acetobacter xylinum by cyclic diguanylic acid. *Nature, 325*(6101), 279-281.

Rossi, S., Laurino, L., Furlanetto, A., Chinellato, S., Orvieto, E., Canal, F., . . . Dei Tos, A. P. (2005). Rabbit monoclonal antibodies: a comparative study between a novel category of immunoreagents and the corresponding mouse monoclonal antibodies. *Am J Clin Pathol, 124*(2), 295-302. doi:10.1309/NR8H-N08G-DPVE-MU08

Saitoh, T., Fujita, N., Hayashi, T., Takahara, K., Satoh, T., Lee, H., . . . Akira, S. (2009). Atg9a controls dsDNA-driven dynamic translocation of STING and the innate immune response. *Proc Natl Acad Sci U S A, 106*(49), 20842-20846. doi:10.1073/pnas.0911267106

Schoggins, J. W., MacDuff, D. A., Imanaka, N., Gainey, M. D., Shrestha, B., Eitson, J. L., . . . Rice, C. M. (2014). Pan-viral specificity of IFN-induced genes reveals new roles for cGAS in innate immunity. *Nature, 505*(7485), 691-695. doi:10.1038/nature12862

Shang, G., Zhu, D., Li, N., Zhang, J., Zhu, C., Lu, D., . . . Gu, L. (2012). Crystal structures of STING protein reveal basis for recognition of cyclic di-GMP. *Nat Struct Mol Biol, 19*(7), 725-727. doi:10.1038/nsmb.2332

Shu, C., Yi, G., Watts, T., Kao, C. C., & Li, P. (2012). Structure of STING bound to cyclic di-GMP reveals the mechanism of cyclic dinucleotide recognition by the immune system. *Nat Struct Mol Biol, 19*(7), 722-724. doi:10.1038/nsmb.2331

Singh, K. V., Kaur, J., Varshney, G. C., Raje, M., & Suri, C. R. (2004). Synthesis and characterization of hapten-protein conjugates for antibody production against small molecules. *Bioconjug Chem, 15*(1), 168-173. doi:10.1021/bc034158v

Spieker-Polet, H., Sethupathi, P., Yam, P. C., & Knight, K. L. (1995). Rabbit monoclonal antibodies: generating a fusion partner to produce rabbit-rabbit hybridomas. *Proc Natl Acad Sci U S A, 92*(20), 9348-9352.

Stetson, D. B., & Medzhitov, R. (2006). Recognition of cytosolic DNA activates an IRF3-dependent innate immune response. *Immunity, 24*(1), 93-103. doi:10.1016/j.immuni.2005.12.003

Storek, K. M., Gertsvolf, N. A., Ohlson, M. B., & Monack, D. M. (2015). cGAS and Ifi204 cooperate to produce type I IFNs in response to Francisella infection. *J Immunol, 194*(7), 3236-3245. doi:10.4049/jimmunol.1402764

Sun, B., Sundstrom, K. B., Chew, J. J., Bist, P., Gan, E. S., Tan, H. C., . . . Ooi, E. E. (2017). Dengue virus activates cGAS through the release of mitochondrial DNA. *Sci Rep, 7*(1), 3594. doi:10.1038/s41598-017-03932-1

Sun, L., Wu, J., Du, F., Chen, X., & Chen, Z. J. (2013). Cyclic GMP-AMP synthase is a cytosolic DNA sensor that activates the type I interferon pathway. *Science, 339*(6121), 786-791. doi:10.1126/science.1232458

Sun, W., Li, Y., Chen, L., Chen, H., You, F., Zhou, X., . . . Jiang, Z. (2009). ERIS, an endoplasmic reticulum IFN stimulator, activates innate immune signaling through dimerization. *Proc Natl Acad Sci U S A, 106*(21), 8653-8658. doi:10.1073/pnas.0900850106

Takeuchi, O., Kawai, T., Muhlradt, P. F., Morr, M., Radolf, J. D., Zychlinsky, A., . . . Akira, S. (2001). Discrimination of bacterial lipoproteins by Toll-like receptor 6. *Int Immunol, 13*(7), 933-940.

Takeuchi, O., Sato, S., Horiuchi, T., Hoshino, K., Takeda, K., Dong, Z., . . . Akira, S. (2002). Cutting edge: role of Toll-like receptor 1 in mediating immune response to microbial lipoproteins. *J Immunol, 169*(1), 10-14.

Tanaka, Y., & Chen, Z. J. (2012). STING specifies IRF3 phosphorylation by TBK1 in the cytosolic DNA signaling pathway. *Sci Signal, 5*(214), ra20. doi:10.1126/scisignal.2002521

Tonegawa, S. (1983). Somatic generation of antibody diversity. *Nature, 302*(5909), 575-581.

Vance, R. E. (2016). Cytosolic DNA Sensing: The Field Narrows. *Immunity, 45*(2), 227-228. doi:10.1016/j.immuni.2016.08.006

Wassermann, R., Gulen, M. F., Sala, C., Perin, S. G., Lou, Y., Rybniker, J., . . . Ablasser, A. (2015). Mycobacterium tuberculosis Differentially Activates cGAS- and Inflammasome-Dependent Intracellular Immune Responses through ESX-1. *Cell Host Microbe, 17*(6), 799-810. doi:10.1016/j.chom.2015.05.003

Watson, R. O., Bell, S. L., MacDuff, D. A., Kimmey, J. M., Diner, E. J., Olivas, J., . . . Cox, J. S. (2015). The Cytosolic Sensor cGAS Detects Mycobacterium tuberculosis DNA to Induce Type I Interferons and Activate Autophagy. *Cell Host Microbe, 17*(6), 811-819. doi:10.1016/j.chom.2015.05.004

Weber, J., Peng, H., & Rader, C. (2017). From rabbit antibody repertoires to rabbit monoclonal antibodies. *Exp Mol Med, 49*(3), e305. doi:10.1038/emm.2017.23

Witte, G., Hartung, S., Buttner, K., & Hopfner, K. P. (2008). Structural biochemistry of a bacterial checkpoint protein reveals diadenylate cyclase activity regulated by DNA recombination intermediates. *Mol Cell, 30*(2), 167-178. doi:10.1016/j.molcel.2008.02.020

Woodward, J. J., Iavarone, A. T., & Portnoy, D. A. (2010). c-di-AMP secreted by intracellular Listeria monocytogenes activates a host type I interferon response. *Science, 328*(5986), 1703-1705. doi:10.1126/science.1189801

Wu, J., Sun, L., Chen, X., Du, F., Shi, H., Chen, C., & Chen, Z. J. (2013). Cyclic GMP-AMP is an endogenous second messenger in innate immune signaling by cytosolic DNA. *Science, 339*(6121), 826-830. doi:10.1126/science.1229963

Wu, J. J., Li, W., Shao, Y., Avey, D., Fu, B., Gillen, J., . . . Zhu, F. (2015). Inhibition of cGAS DNA Sensing by a Herpesvirus Virion Protein. *Cell Host Microbe, 18*(3), 333-344. doi:10.1016/j.chom.2015.07.015

Yin, Q., Tian, Y., Kabaleeswaran, V., Jiang, X., Tu, D., Eck, M. J., . . . Wu, H. (2012). Cyclic di-GMP sensing via the innate immune signaling protein STING. *Mol Cell, 46*(6), 735-745. doi:10.1016/j.molcel.2012.05.029

Yokoyama, W. M., Christensen, M., Dos Santos, G., Miller, D., Ho, J., Wu, T., . . . Neethling, F. A. (2013). Production of monoclonal antibodies. *Curr Protoc Immunol, 102*, Unit 2 5. doi:10.1002/0471142735.im0205s102

Yu, X., Cai, B., Wang, M., Tan, P., Ding, X., Wu, J., . . . Wang, R. F. (2016). Cross-Regulation of Two Type I Interferon Signaling Pathways in Plasmacytoid Dendritic Cells Controls Anti-malaria Immunity and Host Mortality. *Immunity, 45*(5), 1093-1107. doi:10.1016/j.immuni.2016.10.001

Zhang, X., Shi, H., Wu, J., Zhang, X., Sun, L., Chen, C., & Chen, Z. J. (2013). Cyclic GMP-AMP containing mixed phosphodiester linkages is an endogenous high-affinity ligand for STING. *Mol Cell, 51*(2), 226-235. doi:10.1016/j.molcel.2013.05.022

Zhang, X., Wu, J., Du, F., Xu, H., Sun, L., Chen, Z., . . . Chen, Z. J. (2014). The cytosolic DNA sensor cGAS forms an oligomeric complex with DNA and undergoes switch-like conformational changes in the activation loop. *Cell Rep, 6*(3), 421-430. doi:10.1016/j.celrep.2014.01.003

Zhang, Y., Yeruva, L., Marinov, A., Prantner, D., Wyrick, P. B., Lupashin, V., & Nagarajan, U. M. (2014). The DNA sensor, cyclic GMP-AMP synthase, is essential for induction of IFN-beta during Chlamydia trachomatis infection. *J Immunol, 193*(5), 2394-2404. doi:10.4049/jimmunol.1302718

Zhong, B., Yang, Y., Li, S., Wang, Y. Y., Li, Y., Diao, F., . . . Shu, H. B. (2008). The adaptor protein MITA links virus-sensing receptors to IRF3 transcription factor activation. *Immunity, 29*(4), 538-550. doi:10.1016/j.immuni.2008.09.003